PHYSICAL REVIEW B VOLUME 22, NUMBER 6 15 SEPTEMBER 1980

Self-consistent linearized augmented-plane-wave study of the electronic structure and superconductivity of fcc lanthanum under pressure

Warren E. Pickett*
Department of Physics and Astronomy, Northwestern University, Evanston, Illinois 60201

A. J. Freeman
Department of Physics and Astronomy, Northwestern University, Evanston, Illinois 60201
and Argonne National Laboratory, Argonne, Illinois 60439

D. D. Koelling
Argonne National Laboratory, Argonne, Illinois 60439
(Received 16 October 1979)

We report the results of a linearized augmented-plane-wave calculation of the electronic structure of fcc La at three lattice constants corresponding to ambient pressure, 50, and 120 kbars. The Kohn-Sham-Gáspar approximation for exchange and correlation is used and the potential is allowed a fully non-muffin-tin form. The f bands lie $\sim$2–2.5 eV above the Fermi level and are $\sim$1 eV wide, resulting in a very small (0.05 electrons) localized f occupation. Under pressure the f bands rise and broaden appreciably, resulting in only a slight increase in f occupation. The rigid-muffin-tin approximation for the electron-phonon interaction λ overestimates the superconducting transition temperature T_c by 40%, but we find that the drastic increase in T_c under pressure can be attributed primarily to changes in the electronic stiffness η. Structural transitions which occur at 25 and 53 kbars may be related to changes in Fermi-surface topology which we find to occur approximately at these pressures.

I. INTRODUCTION

The observation in lanthanum[1] of a high superconducting transition temperature T_c and its large pressure derivative dT_c/dP has led to wide speculation that a pairing mechanism involving f electrons is responsible. Under pressure, T_c rises sharply from 6 K at ambient pressure and saturates at a value of nearly 13 K around 200 kbars, as shown in Fig. 1. Two separate questions arise: (i) Why is La a high-T_c superconductor at all, since the isoelectronic elements Sc and Y are not good superconductors? (ii) What is the cause of the large pressure derivative, $dT_c/dP \simeq 1$ K/10 kbar, which is among the largest known for superconductors?

From Fig. 1, the slope dT_c/dP is seen to show structure at 25 and 53 kbars. In addition, Balster and Wittig[1] have measured a concomitant anomaly in the low-temperature electrical resistivity at 53 kbar. As La is known[2] to be fcc at room temperature in a wide pressure range around 53 kbar, they have proposed that these anomalies arise from an isostructural (fcc $\longleftrightarrow$ fcc) phase transition which terminates at a critical point below room temperature. Especially considering the decrease in dT_c/dP by a factor of 4 (Ref. 1) at this transition, this revives questions concerning the complex interrelation of lattice instability, phonon softening, and high-temperature superconductivity.

The superconductivity of La was attributed by Kondo[3] and many others[4-5] to f-electron mechanisms of various kinds, with the large pressure derivative of T_c resulting from variation with pressure of the energy of the f state. The explanation in terms of f-electron states lying above, but very close to, the Fermi level E_F was also supported by other peculiarities observed in La. The temperature dependence of the magnetic susceptibility[6] was interpreted to be due to an effective localized moment of one-half Bohr magneton, and the Knight shift, also normally temperature independent, was found[7] to increase by 20% in cooling from room temperature to 1.5 K. The linear specific-heat coefficient[8] was found to be very large and the thermal-expansion coefficient[9] was found to be negative in certain temperature regions. These phenomena all seemed to suggest the occurrence of significant $4f$-electron character in La, and it has been argued[1,10] that La must be a "$4f$-band" metal. In addition, the low melting point of La had led Matthias *et al.*[11] to postulate an f-electron concentration of 0.7 electrons/atom.

However, the development of reliable tunnel junctions led to the unambiguous assignment of La as a relatively strong-coupling d-electron superconductor,[12-15] with electron-phonon coupling constant $\lambda \simeq 0.8-0.9$. While this partially accounts for the large electronic specific heat, which is enhanced by the factor $(1+\lambda)$, it still leaves the possibility that the pressure enhancement of T_c is related to f character in the electronic structure. Ratto, Coqblin, and Galleani[5] have attributed

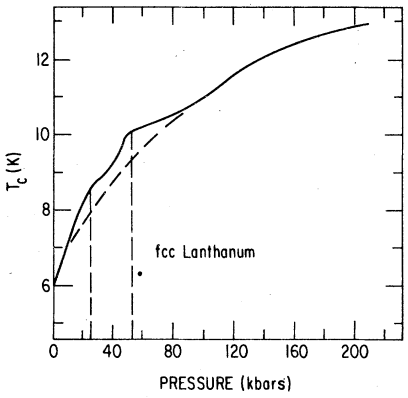

FIG. 1. Superconducting transition temperature T_c versus pressure from Ref. 1 and references therein. The dashed line merely interpolates smoothly between the low- and high-pressure regimes.

the increase in T_c to the "squeezing out" of local f-electron character with its pair-breaking tendency, as the f level *rises* under pressure. Weling,[16] on the other hand, has shown that if the f level *lowers* under pressure, the increased polarizability arising from virtual excitations into the f level softens the phonon spectrum and enhances T_c. Thus the f enigma remains, and central questions which must be addressed involve the position and volume dependence of the f levels in La.

There has been relatively little theoretical effort given to determining the electronic structure of La. This is no doubt related to the scarcity of experimental data available for comparison, itself a result of the two-phase (dhcp + fcc) nature of La at low pressures and at room temperature and below. Kmetko[17] reported a self-consistent nonrelativistic determination of f-electron charge *reduction* under pressure in fcc La using the augmented-plane-wave (APW) method. Earlier, Fleming *et al.*[18] and Myron and Liu[19] had presented non-self-consistent relativistic APW (RAPW) results for the band structures and Fermi surfaces of dhcp and fcc La, respectively. More recently, Glötzel and Fritsche[20] have studied the pressure dependence of the electronic structure of fcc La using a semirelativistic rigorous cellular method, and Glötzel[21] has reported ground-state properties calculated self-consistently utilizing the linear-muffin-tin-orbital (LMTO) method. Very recently, Takeda and Kübler[22] have applied a self-consistent form of the semirelativistic (SR) linearized APW (LAPW) scheme in the atomic-sphere approximation (ASA) to fcc La.

In this paper, we describe the results of a self-consistent (SC) *relativistic* LAPW study of the band structure of fcc La at three values of the lattice constant. The method is described in Sec. II. An important feature of this approach, especially in view of the care which is necessary when treating f states, is that few restrictions (i.e., constraints) are built in; for example, the charge density and the resulting self-consistent potential are allowed a general (i.e., non-muffin-tin) form, and important relativistic effects are included either exactly (mass-velocity and Darwin terms) or nonperturbatively (spin-orbit interaction).

The main features of the electronic structure of La under pressure, including the self-consistent charge density and character of the d and f states, are presented and discussed in some detail in Sec. III. The *localized* f-electron charge is found to be ~0.05 electrons and to increase somewhat under pressure, despite the fact that the center of the f bands, which lies 2.5–3 eV above E_F, increases with pressure. This increase in f-electron charge is due to increased hybridization as the bands (sp, d, and f) broaden under pressure.

The band-structure results of Sec. III are used in Sec. IV to interpret the 25-kbars phase transition[23] and the 53-kbars phase transition which occurs at low temperature. The theoretically observed behavior of the bands under pressure strongly suggests a Lifshitz-Dagens[24,25] structural instability due to a strongly d-f hybridized band crossing E_F in both pressure ranges. In Sec. V it is shown that the rigid-muffin-tin approximation (RMTA) for the electron-phonon matrix element accounts for the magnitude and, most likely, the pressure enhancement of T_c, although the RMTA itself is less justifiable here (because of the expanded d function) than in the later transition elements where it has been applied with more success. The generalized susceptibility, and especially its implications for phonon anomalies and structural stability, is examined in Sec. VI. We conclude in Sec. VII with a discussion of the present theoretical understanding of La.

II. METHOD OF CALCULATION

Since detailed discussions of our calculational procedures have been given elsewhere,[26-29] only a descriptive review will be presented here. This will serve to orient the reader as well as to provide a basis for discussing discrepancies between the present results and those obtained previously by other means. The discussion is separated into three parts: (i) the secular equation and its solution, (ii) the determination of the charge density and resulting screening potential necessary for the self-consistency loop, and (iii) the treatment of the spin-orbit interaction at the final step.

A. The secular equation

Ideally one would like to solve the Dirac equation for a relativistic electron in a periodic potential V. The basis set $\{\Phi\}$ is constructed in the usual APW dual representation,[29] as plane waves outside nonoverlapping spheres of radius R and as solutions of a spherically averaged potential inside the spheres. This results in coupled first-order differential equations for the radial functions g_κ, f_κ, in terms of which the basis APW is given by[29] (in standard notation)

$$\Phi_{\kappa\mu}=\begin{pmatrix} g_\kappa \chi_{\kappa\mu} \\ -if_\kappa \sigma_r \chi_{\kappa\mu} \end{pmatrix}, \quad r<R. \tag{1}$$

Here κ, μ are the relativistic quantum numbers for the central-field problem, and $g(f)$ is the radial function describing the large (small) component. For each value of the nonrelativistic orbital quantum number l, there are two values of κ corresponding to total angular momentum $j=l+\frac{1}{2}$ and $j=l-\frac{1}{2}$.

Koelling and Harmon[26] have shown that in many cases it is desirable to retain spin as a "good" quantum number, both for computational and physical reasons. This can be done by forming a j-weighted average g_l, for a given l, of the radial solutions g_κ, and subsequently dropping a κ-dependent term in the differential equation for g_κ which corresponds to spin-orbit coupling. In effect this reduces the solution of the radial problem to the simplicity of the corresponding nonrelativistic problem while including the important Darwin and mass-velocity corrections. The spin-orbit interaction, in addition to being generally smaller, serves primarily to split degenerate states (or states of similar l character) at points, or along lines, of high symmetry. The spin-orbit corrections are often negligible; for La, however, they have been included in a final variational procedure, described in Sec. II C below.

The energy-dependent secular equation is linearized following Koelling and Arbman.[27] The radial solution $g_l(E)$ is replaced by a linear combination of the solution $g_l(E_l)$ at a fixed energy E_l and the energy derivative $\dot{g}_l(E_l)$, also evaluated at E_l. The linear combination is fixed by requiring both the basis function and its derivative to be continuous across the sphere boundary. The resulting technique has been found to be quite accurate (see below) over a range of several tenths of a Rydberg around $E=E_l$. In Table I the input parameters for the calculations for La are presented.

The periodic potential $V(r)$ is restricted only to have a form consistent with the symmetry of the crystal. For La, it is expanded in the unit cell

TABLE I. Input parameters for LAPW calculations for La at three lattice constants (a): approximate corresponding pressure (P), muffin-tin-sphere radius (R), maximum possible sphere radius $a/2\sqrt{2}$, and the energies E_l about which the basis APW's are linearized. Distances are in atomic units and energies are in rydbergs. The Fermi energy E_F is included as a reference of energy for E_l.

a	P (kbars)	R	$\frac{a}{2\sqrt{2}}$	$E_{l\neq 1}$	E_1	E_F
10.0348	0	3.4924	3.5490	0.400	0.550	0.423
9.4760	~50	3.2808	3.3502	0.600	0.900	0.522
9.0340	~120	3.1799	3.1940	0.750	1.100	0.601

at the origin in the dual representation

$$V(\vec{r})=\begin{cases} \sum_{\vec{K}} V_{\vec{K}} e^{i\vec{K}\cdot\vec{r}}, & r>R \\ \sum_{l} V_l(r) K_l(\hat{r}), & r<R. \end{cases} \tag{2}$$

Here K_l denotes the Kubic harmonics of full cubic (Γ_1) symmetry, and only the $l=0$, 4, and 6 harmonics are retained. Higher-l harmonics are expected to give negligible corrections. The Fourier expansion in the interstitial region is carried to far more reciprocal-lattice ($\vec{K}$) stars (90) than is actually necessary for convergence. Using these criteria, the truncation of these representations leads to a maximum discontinuity in V at the sphere radius of 5 mRy for La. For any practical purpose this representation of the potential can be considered to be unrestricted.

The crystal eigenfunctions are expanded as a linear combination of the basis LAPW's, with the coefficients determined variationally. In addition to the usual kinetic-energy and spherical potential-energy matrix elements, it is necessary to calculate the matrix elements of warping and nonspherical terms in the potential in Eq. (2). The procedure is straightforward and has been described elsewhere.[29]

It only remains to fix the number of basis functions to be used in the secular equation. This is done separately for each k point by including all LAPW's corresponding to the condition $|\vec{k}+\vec{K}|<K_{\max}$. To get reasonable convergence of the f bands (see below) we find $RK_{\max}=8$ to be a useful criterion, corresponding to ~55 LAPW's. For $RK_{\max}\geq 9$ (corresponding to 70–80 LAPW's) approximate linear dependence of the basis set can sometimes lead to numerical difficulties in the Choleskii decomposition of the overlap matrix.

B. Construction of the general potential

The charge density ρ is expanded in a straight-

forward manner in a dual representation in parallel with the potential and the basis functions, again retaining $l=0$, 4, and 6 Kubic harmonic terms inside the sphere. This charge density is used to construct the screening potential, consisting of the electrostatic potential which satisfies Poisson's equation and an exchange-correlation potential in the local density approximation. All the results described here were obtained using the Kohn-Sham-Gásper ($\alpha=\frac{2}{3}$) $\rho^{1/3}$ approximation, with no explicit additional correlation correction. Using a correlation potential corresponding to a (perhaps density dependent) α greater than $\frac{2}{3}$ would lead to slightly more localized f states (but see Sec. VII).

The grid of k points used to calculate ρ in the first ~12 iterations consisted of equally weighted points at the center of mass 16 equal-volume tetrahedra in the irreducible Brillouin zone (IBZ). For the final ~6–8 iterations to self-consistency, each tetrahedron was subdivided into eight equal-volume tetrahedra. The centers of mass of these (128 equally weighted) tetrahedra made up the final k-point grid. None of these points lie on symmetry directions so the possible problem of degenerate states as E_F never arises.

C. Spin-orbit interaction

The spin-orbit (SO) interaction was ignored (as described in Sec. II A) in the iterations to self-consistency. This is a reasonable approximation in most systems since the effect of SO corrections is primarily to split degeneracies along symmetry lines rather than to cause a net shift of states to higher or lower energy. In addition, in La the SO corrections are rather small, as will be discussed below.

The observation that the SO interaction only splits degeneracies suggests an approach in which SO is treated in a separate variation within a subset of bands, which in practice will consist of only the bands in the energy region of interest (near E_F). This method has been discussed in detail elsewhere[28] so only a descriptive review will be given here.

Suppose the $N\times N$ secular equation described in Sec. II A has been solved for the lowest M eigenstates ($M<N$)—a common numerical practice to save computational time when all eigenstates are not desired. For La, the region of interest includes s (1), d (5), f (7), and perhaps p (3) bands so that $M\simeq 15$. (Recall that $N\approx 60$ has been used for the secular equation.) Within this M subspace, the SO matrix elements are evaluated and the effective Hamiltonian is rediagonalized, yielding approximate (but usually excellent) fully relativistic eigenstates and eigenvalues.

The advantage of this procedure is that spin is retained as a good quantum number as long as possible. This is preferable physically, of course, but also is computationally very desirable, since it is only necessary to handle a $2M\times 2M$ complex matrix in the final stage rather than a $2N\times 2N$ (120×120 in this case) complex matrix throughout the SC procedure.

This scheme has been found to be very accurate for determining eigenvalues in La and Ce (Ref. 30) as well as in transition metals.[28] The primary restriction seems to be that the resulting relativistic eigenfunctions are required for a given l to have the same radial dependence for $j=l\pm\frac{1}{2}$; i.e., there is only one radial function g_l for each l rather than the two functions g_κ from the full relativistic treatment. This restriction may be more serious in very heavy elements.[28]

To include the SO interaction in the LAPW method it is necessary to evaluate the quantities[28]

$$\xi_l^0=\int_0^R dr\,r^2\left(\frac{g_l}{2Mcr}\right)^2\frac{r\,dV}{dr}\,, \tag{3a}$$

$$\xi_l^1=\int_0^R dr\,r^2\left(\frac{g_l}{2Mcr}\right)\left(\frac{\dot{g}_l}{2Mcr}\right)\frac{r\,dV}{dr}\,, \tag{3b}$$

$$\xi_l^2=\int_0^R dr\,r^2\left(\frac{\dot{g}_l}{2Mcr}\right)^2\frac{r\,dV}{dr}\,, \tag{3c}$$

which provide the magnitude of the SO interaction $\xi_l(E)$:

$$\xi_l(E)\cong\xi_l^0+2(E-E_l)\xi_l^1+(E-E_l)^2\xi_l^2\,. \tag{4}$$

In Eq. (3), dV/dr is the radial derivative of the spherical part of the potential and $2M\equiv 2m+(E_l-V)/c^2$. The resulting values for La at three lattice constants are given in Table II up to $l=3$; for higher l, the ξ_l^i are less than 5×10^{-6}. The $l=1$ SO parameter is large (~55 mRy) but enters into eigenvalues in the region of interest

TABLE II. Values of the spin-orbit parameters defined in Eq. (3). The three lattice constants are $a_0=10.0378$, $a_1=9.4760$, $a_2=9.0340$ a.u.

		ξ_l^0(mRy)	ξ_l^1	ξ_l^2(mRy^{-1})	$\xi_l(E_F)$ (mRy)
$l=1$	a_0	48.6	−9.2	1.7	51.0
	a_1	59.5	−8.7	1.3	66.3
	a_2	65.9	−8.6	1.1	74.8
$l=2$	a_0	2.7	2.0	1.5	2.6
	a_1	3.4	2.0	1.2	3.1
	a_2	3.9	2.1	1.1	3.3
$l=3$	a_0	1.5	3.2	6.9	1.4
	a_1	2.1	3.3	5.3	1.6
	a_2	2.5	3.1	3.9	1.7

with negligible weight because the wave functions have very little p character. The $l=2,3$ SO parameters are much smaller than the 20-mRy value estimated by Takeda and Kübler.[22] Note that the spin-orbit parameter at the Fermi energy increases with pressure. This is consistent with the electron spending a greater time near the nucleus as the volume is reduced.

III. RESULTS

Self-consistent calculations have been carried out for lattice constants of 10.0378, 9.4760, and 9.0340 a.u. At room temperature these values correspond approximately to ambient (0), 50, and 120 kbar pressure,[2] respectively. Although low-temperature data of lattice constant versus pressure are not available, the zero-pressure thermal-expansion coefficient[10] suggests pressure differences between 0 and 300 K of only ~2 kbars. In the following, the various results obtained at the three lattice constants will be discussed concurrently.

A. Band structure

The band structures of La along symmetry directions for the three lattice constants are shown in Fig. 2. The spin-orbit interaction has been included in the eigenvalues plotted here to provide a realistic indication of the size and importance of SO corrections. However, since the SO effects are rather small, it is more transparent physically to present the discussion in terms of the corresponding band structures before introducing the SO interaction. This also facilitates comparison with other calculations which neglect SO effects.

Consider first the ambient-pressure band structure in Fig. 2(a). At the zone center, only the Γ_1 s-derived state lies below E_F. At progressively higher energies the eigenvalues are $\Gamma_{2'}$, $\Gamma_{25'}$, Γ_{15}, Γ_{25}, and Γ_{12}. The $\Gamma_{25'}$ and Γ_{12} states arise from atomic d states while $\Gamma_{2'}$, Γ_{15}, and Γ_{25} are f states. Thus the d and f states are intertwined at the zone center, and indeed throughout the zone, as will become evident. Under applied pressure the ordering of states at Γ is unchanged.

In the fcc lattice, Γ is a convenient point to use in discussing relative d-f character and separation because the states are completely decoupled. Another such point is the X point $[(1,0,0)2\pi/a]$, while at other high-symmetry points the separation of d and f character is more ambiguous. Indeed, for a certain volume surrounding the X point the f bands are well separated from the other bands, and, in addition, they are nearly dispersionless there (Fig. 2). These observations suggest the use of the Γ and X points in characterizing the f-band center C_f and width W_f. We take the extrema to define the bandwidth, e.g., $W_f(\Gamma)=E(\Gamma_{25})-E(\Gamma_{2'})$. The band center C_f is defined as the mean of the seven eigenvalues and is measured relative to E_F. The behavior of C_f and W_f under pressure is given in Table III. The center of the f band rises under pressure monotonically, relative to E_F, from 2.2 to 2.7 eV [using the average of $C_f(\Gamma)$ and $C_f(X)$]. Surprisingly, the band width $W_f(\Gamma)$ at Γ nearly doubles under pressure, from 1.15 to 2.05 eV, while $W_f(X)$ remains essentially unchanged at the value 0.55 ± 0.05 eV. This paradox brings into question the origin of the f bandwidth at various points in the zone. At least three possible sources arise: (i) intrinsic bandwidth, resulting from f-f nearest-neighbor overlap, (ii) hybridization bandwidth, induced in this case primarily by d-f hybridization, and (iii) crystal-field bandwidth, arising from the cubic crystal field felt by the localized f electrons. It is not clear *a priori* to what extent (ii) and (iii) are independent. This interesting problem will be discussed further in Sec. VI.

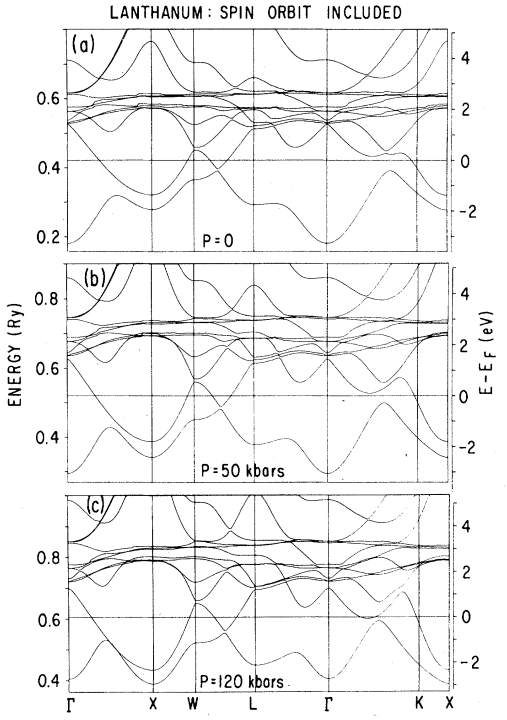

FIG. 2. Fully relativistic dispersion relations for fcc La along symmetry lines for pressures of 0, 50, and 120 kbars from 180 first-principles points (i.e., no interpolation). Spin-orbit splittings are visible, e.g., at Γ. The "kinks" in the flat f bands arise from the lack of complete convergence of these bands; the eigenvalues on the high side of a kink are up to 4 mRy from convergence.

TABLE III. Variation with lattice constant a of the f- and d-band center C and width W at the Γ and X points. Both C and W are given in mRy and C is measured from the Fermi level. To provide comparison the percentage increase Δ under pressure is given in the last column.

a(a.u.)	=10.0378	9.4670	9.0340	Δ(%)
$C_f(\Gamma)$	159	179	192	21
$C_f(X)$	168	191	208	24
$W_f(\Gamma)$	86	116	149	73
$W_f(X)$	37	39	44	19
$C_d(\Gamma)$	181	205	228	26
$C_d(X)$	214	261	310	45
$W_d(\Gamma)$	181	221	260	44
$W_d(X)$	633	766	891	41

Also listed in Table III are the center C_d and width W_d of the d bands as determined from the Γ and X points. The d-band center rises from 2.7 to 3.7 eV above E_F under pressure, using the average of $C_d(\Gamma)$ and $C_d(X)$. The d bandwidth, conventionally defined using the X point value $W_d(X)$, increases from 8.6 to 12.1 eV, a change by more than 40%. A particularly interesting feature is that, for the maximum pressure $P \approx 120$ kbars considered here, the lowest d state (at X) lies lower than the s state (Γ_1) at Γ. Since the *occupied* d-band region $E_F - E(X_1)$ increases from 2.0 to 3.0 eV under pressure while the occupied s-band region decreases, we expect an s-to-d shift of electrons under pressure which is confirmed by the partial density-of-states results given below. Finally we note that band 2 along the Σ direction drops below E_F under pressure. We return to this important point in Sec. IV.

B. Density of states and charge density

The density of states $N(E)$ at each of the three lattice constants is shown in Fig. 3. The Fermi level is found to lie near a peak arising from primarily d-like states in band 2. The density-of-states peak at a binding energy of 1.1 eV at ambient pressure is in good agreement with the 0.9 $\pm$ 0.2 eV value obtained from x-ray photoelectron-emission spectroscopy.[31] The huge peaks coming from the f bands at $E = 2$–3 eV lie far off the scale of Fig. 5 and have not been shown. The dominant effect of pressure on $N(E)$ is the broadening of the bands and the resulting *decrease* of $N(E)$ in most regions of energy. The density of states at E_F, $N(E_F)$, decreases from 27.5 to 21.4 states/Ry atom in the pressure range considered here and should have measurable experimental consequences, for example, in the specific heat and susceptibility.

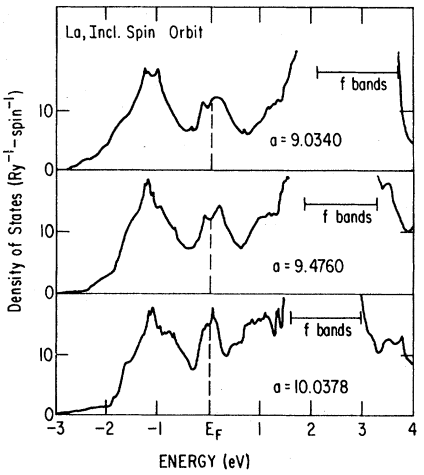

FIG. 3. Total density-of-states curves for fcc La for pressures (increasing upward) of 0, 50, and 120 kbars. The huge peak at 2–3 eV due to the f bands goes far off the scale and has not been shown.

To facilitate a more complete description of the electronic structure of La, the angular-momentum-projected partial density of states $N_l(E)$ inside the spheres was also computed through $l = 4$. The d and f components were also decomposed according to cubic irreducible representations (Γ_{12}, $\Gamma_{25'}$) and ($\Gamma_{2'}$, Γ_{15}, Γ_{25}) for $l = 2$ and $l = 3$, respectively. The integral of the occupied partial density of states gives in turn the amount of charge Q_l inside the sphere with a particular angular momentum character. The "interstitial density of states" can be defined as $N_{\text{int}}(E) = N(E) - \Sigma_l N_l(E)$, and similarly for the interstitial charge Q_{int}. These quantities have been listed in Table IV. The density of states was calculated with the tetrahedron method, using 1024 tetrahedra in the IBZ. First-principles eigenvalues were calculated at the vertices of each tetrahedron (totaling 293 distinct points) and the energy was interpolated linearly within the tetrahedron. This procedure results in sufficiently accurate results with modest computational effort and eliminates uncertainties which arise from the use of Fourier-series representations.

Both the charge and density of states are dominated by d contributions, with the $\Gamma_{25'}$ component being roughly twice as large as the Γ_{12} component in each case. The pressure dependence of $N_l(E_F)$ is dominated by the band broadening and concomitant lowering of $N_l(E_F)$ values as mentioned above, with the exception of the f Γ_{15} component which increases markedly. The pressure behavior of the charge consists of a moderate shift of s and p to d and f. The variations in the interstitial charge given in Table IV is a direct consequence of the fact that the fraction of cell volume assigned

TABLE IV. Angular-momentum-decomposed density of states at E_F, $N_l(E_F)$ and corresponding electronic charges Q_l within the APW sphere. "Int." denotes the interstitial contribution. For d and f contributions the specific cubic irreducible representations are given. Lattice constants 10.0378, 9.4760, 9.0340 are denoted by a_0, a_1, a_2, respectively, $N_l(E_f)$ is measured in (states/Ry atom) and Q_l is given in electrons. The values in parentheses are from nonrelativistic self-consistent APW calculations of Kmetko (Ref. 17); only total $l=2,3$ values were reported by Kmetko.

	a	s	p	$d(\Gamma_{25'})$	$d(\Gamma_{12})$	$f(\Gamma_2')$	$f(\Gamma_{25})$	$f(\Gamma_{15})$	g	Int.	Total
$N_l(E_F)$	a_0	0.55	2.30	10.95	4.55	0.82	0.23	1.19	0.07	6.81	27.47
	a_1	0.39	1.58	8.29	3.74	0.75	0.25	1.20	0.07	5.77	22.04
	a_2	0.55	1.22	7.02	4.28	0.85	0.34	2.03	0.09	4.99	21.37
Q_l	a_0	0.41	0.15	0.99	0.55	0.03	0.02	0.05	0.00	0.80	3.00
		(0.29)	(0.11)	(1.34)			(0.55)			(0.67)	
	a_1	0.34	0.12	1.01	0.56	0.04	0.02	0.07	0.01	0.83	3.00
		(0.23)	(0.13)	(1.66)			(0.38)			(0.65)	
	a_2	0.29	0.10	1.06	0.61	0.05	0.03	0.10	0.01	0.75	3.00

to the interstitial region (or to the sphere) is different at each lattice constant (see Table I). From Table IV, we find that the amount of f electrons increases from 0.10 to 0.18 under pressure. It will be shown below that these values are a considerable overestimate of any *localized f* charge which may be present.

Figure 4(a) shows the self-consistent radial densities σ_4 and σ_6 for the $P=0$ and 120 kbar lattice constants, with $\sigma_l = 4\pi r^2 \rho_l(r)$ defining the radial charge density. In the expansion of ρ inside the sphere, ρ_l is multiplied by K_l, shown in Fig. 4(b). It can be seen that the largest nonspherical correction is σ_4, which is negative along the second-neighbor direction [100] and positive along [111]. It can be seen from the small-r behavior of

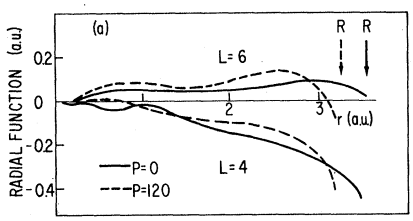

LANTHANUM CHARGE DENSITY

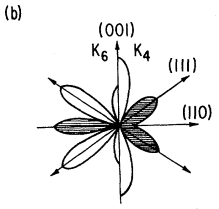

FIG. 4. The nonspherical radial charge densities (a) for $L=4$, 6 at ambient pressure and 120 kbars. The cubic harmonics for $L=4$, 6 in the (110) plane (b) with shading representing negative values.

σ_4 that at ambient pressure there is an excess t_{2g} population which washes out with pressure. This observation is consistent with the data of Table IV. There is no lobe of K_4 directed toward the nearest neighbor (NN) in the fcc lattice. The $l=6$ term, which arises almost entirely from f functions, is negative along [110] at ambient pressure, indicating no tendency to bond with NN atom. The downturn in σ_6 near the sphere radius at 120 kbars is an effect of overlapping atomic charge rather than a tendency toward bonding. Both nonspherical corrections V_4, V_6 to the potential (not pictured) are negligible for $r < 2$ a.u. but rise sharply at larger radii, becoming 0.3 Ry (0.4 Ry) at the APW sphere at 0 (120) kbars.

The effects of non-muffin-tin corrections to the potential on the eigenvalues at Γ and X (for $a = 9.0340$) are displayed in Table V. As expected, the corrections arising from both nonspherical and warping terms are small enough to be additive. Generally, the effects on localized states (the f states and the nonbonding d states Γ_{12} at the top of the d band) are in the range 0–3 mRy, with the exception of 7-mRy shift of the lowest f band $\Gamma_{2'}$. The effects on the bonding d states at X are as large as 22 mRy and are quite significant for reproducing details in a self-consistent calculation accurately.

The behavior of the $l=2,3$ radial functions at E_F is shown in Fig. 5. The d function is typical of a bonding state at the bottom of the band and peaks midway between NN atoms. The f function is rather unusual. It does show a relative maximum at the position ($r \approx 0.75$ a.u.) where the $4f$ function peaks in the rare-earth elements. However, since E_F is more than two bandwidths below the center of the f bands, g_3 at and below E_F is not strictly an atomiclike $4f$ radial function.

TABLE V. Eigenvalues (in mRy) of La ($a = 9.0340$) at Γ and X illustrating the effect of non-muffin-tin corrections to the potential. For the muffin-tin calculation both the warping terms $V_{\vec{K}}$ and nonspherical terms V_4 and V_6 were set to zero. $X(f)$ denotes the f-derived states at X.

	Full LAPW	$V_{\vec{K}} \equiv 0$	$V_4 = V_6 = 0$	Muffin-tin
Γ_1	405	400	404	400
$\Gamma_{2'}$	699	705	701	706
$\Gamma_{25'}$	725	732	730	736
Γ_{15}	769	769	768	768
Γ_{25}	848	848	849	849
Γ_{12}	985	988	984	986
X_1	388	373	381	366
X_3	434	446	438	450
$X(f)$	790	791	791	793
	792	793	793	794
	801	803	801	803
	825	825	825	825
	834	835	835	835

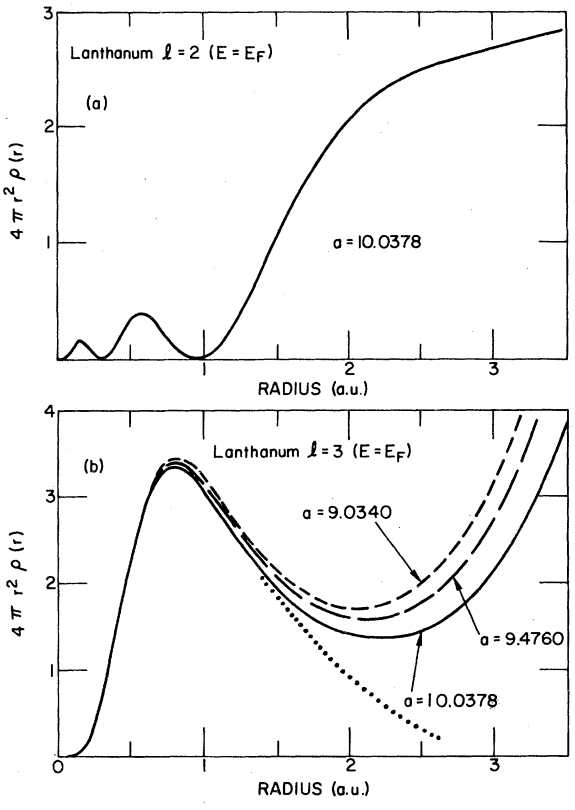

FIG. 5. Plots of the radial wave function (g_l) shape for $l = 2, 3$ out to the sphere radius. In (b) the behavior of the $l = 3$ function under pressure is shown. The dotted line in (b) is a sketch of the behavior of an atomic $4f$ radial function.

Neither does it resemble the $4f$ wave function in the $4f$ bands above E_F (which is much more atomic-like). We find that g_3 increases for $r > 2$ a.u. in much the same manner as occurs in transition metals with lower atomic number, i.e., as the $l = 3$ spherical Bessel function in the expansion of the conduction electron eigenfunction at a similar energy. The "f electrons" described by g_3 therefore are only approximately 50% localized $4f$-like electrons. The character of g_2 and g_3 shown in Fig. 5 will be relevant to the discussion of superconducting properties given below.

C. Comparison with previous calculations

Early band-structure results using a non-SC RAPW method were reported by Myron and Liu[19] for fcc La and by Fleming, Liu, and Loucks[18] for dhcp La. Neither reported details of the band structure in the f-band region, concentrating rather on Fermi-surface topology. The Fermi-surface dimensions and $N(E_F) = 24.8$ Ry^{-1}atom^{-1} reported by Myron and Liu (for lattice constant 10.011 a.u.) are in semiquantitative agreement with our results (see Sec. III D).

Kmetko[17] has reported angular-momentum-decomposed charges from nonrelativistic SC APW calculations in the muffin-tin approximation for fcc La at lattice constants of 9.991 and 9.492 a.u. His results are presented in parentheses in Table IV, and describe a *large* f charge $Q_3 = 0.55$ electrons which *decreases* to 0.38 under 50-kbar pressure. Our results show a rather *small* f charge $Q_3 = 0.10$ which *increases* to 0.13 under 50-kbars pressure, mainly due to increased hybridization. Kmetko used the $X\alpha$ value $\alpha = 0.693$ for exchange and correlation, which is very close to the value of $\alpha = \frac{2}{3}$ used in this work. Since it seems unlikely that the non-muffin-tin corrections we have included could account for much of this discrepancy, the smaller f charge (compared to Kmetko's results) which we find probably is due to relativistic effects which we have included. This is consistent with the expectation that relativistic corrections lower small angular momentum eigenvalues relative to larger angular momentum eigenvalues and as a result shifts charge to lower l values. This trend can be seen as well in the Q_0, Q_1, Q_2 values of Table IV. This makes it apparent that a relativistic theory is essential for a correct description of the electronic structure of La.

Glötzel and Fritsche[20] (GF) have reported non-SC semirelativistic rigorous-cellular-method results for La at zero and 120 kbars (lattice constants were not given). Overall their band structure and its pressure dependence is quite similar

to ours, although the lack of self-consistency inevitably leads to differences in detail. As an example of the degree of agreement shown with our results, GF find $C_f(X) \approx 200$ mRy at zero pressure increasing to ~260 mRy at 120 kbars, compared to our results of 169 and 208 mRy, respectively. Their ambient-pressure value of $N(E_F) = 26.8$ Ry^{-1}atom^{-1} compares favorably with our value of 27.4 Ry^{-1}atom^{-1}. However, their density-of-states curve for 120-kbars pressure is considerably different from what we find, and this is reflected in their 10% lower value of $N(E_F)$. Generally we can conclude that self-consistency is important in describing the electronic structure and its pressure dependence in La.

Glötzel[21] has reported limited results of calculations on fcc La using the ASA adaption of the linear-muffin-tin-orbital method. He finds 0.17 f electrons at zero pressure and a small increase under pressure. Consdering that his definition of f electrons uses an atomic sphere rather than the inscribed sphere we use and that the f radial function is *not* localized for energies at and below E_F [see Fig. 5(b)], his conclusion is in good agreement with our result, shown in Table IV and discussed above. His value for $N(E_F) = 33.6$ Ry^{-1} atom^{-1} is 23% greater than we find and suggests considerable difference in detail between the two calculations.

Takeda and Kübler[22] (TK) recently have reported SC semirelativistic LAPW calculations for fcc La. We find several differences between their results for $a = 10.011$ a.u., neglecting SO, and our corresponding ($a = 10.034$ a.u., no SO) results. TK find f bands which are twice as wide and nearly twice as far above E_F as those shown in Fig. 2. However, their occupied s and d bandwidths are only about 10% wider than found in the present work and their value of $N(E_F) \approx 26$ (Ry atom)$^{-1}$ is similar to our value of 27.4 (Ry atom)$^{-1}$. In two calculations which on the surface would be expected to yield similar results (both are SC semirelativistic LAPW calculations) it is important to understand the cause(s) of the differences.

Considering the well-converged representations of charge density and potential and the careful self-consistency, we believe the only significant inaccuracy in the present calculations come from the linearization of the energy-dependent APW secular equation. The energy parameters E_l have been adjusted to reduce the inaccuracy as much as possible in the region of interest (near E_F and in the f bands). Moreover, by equating the energy parameters to an eigenvalue $E(k)$ we can reproduce the (unlinearized) APW eigenvalue and hence check the error due to linearization. Tests indicate that, for the set of E_l we have chosen (see Table I), the linearization procedure leads to an inaccuracy in the eigenvalues in the f bands and below of less than 2 mRy. For the case of La, it is necessary to have E_1 several tenths of a Rydberg above E_F (nearer the $6p$ resonance) to keep spurious p-derived bands out of the region of interest. (Generally, it is desirable to place E_l near the l resonance, or, if the l resonance is far from E_F, somewhere between E_F and the l resonance.)

The methods used by TK differ from those used in the present study in a number of respects. TK assume a muffin-tin form of potential (ρ, V spherical inside the muffin-tin sphere, constant in interstitial region) and extend it using the "atomic-sphere approximation" (ASA) to overlapping spheres with volume equal to the atomic volume. This has been found to be a reasonable approximation in elemental transition metals, but it is relatively untested in f-band systems. Certainly the non-muffin-tin corrections (discussed in the preceding section) are not large enough to account for the discrepancies. No doubt more severe is the use by TK of only 27 APW's in the secular equation; we have found that as many as 55–60 APW's may give f bands which are still 4 mRy from the converged value for certain wave vectors. If only 27 LAPW's are used in our secular equation, we find the $\Gamma_{2'}$, and Γ_{15}, and Γ_{25} eigenvalues are too high by 93, 76, and 31 mRy, respectively. The d eigenvalues $\Gamma_{25'}$ and Γ_{12} are affected less, being too high by 4 and 10 mRy, respectively, while the Γ_1 eigenvalue is unchanged to 0.1 mRy. The f eigenfunctions, and to a lesser extent the d eigenfunctions, are quite poorly represented by only 27 LAPW's and will contribute errors in the charge density. Still another source of inaccuracy in the TK results is their utilization of a moment method of generating an approximate charge density, which is then used to determine the potential. Unfortunately, we are not aware of any tests of this moment method which would allow a quantitative estimate of its accuracy.

Finally we note two other differences in these SC LAPW calculations. The linearization method used by TK augments with radial functions at two energies (which are not reported with their results for La), whereas the method we have used utilizes the radial function and its energy derivative at a single energy. However, for reasonable choices of the energy parameters, the two methods should give very similar results. The last difference is that TK used the Hedin-Lundqvist approximation[22] for correlation. In both sp metals and d metals this leads to very minor differences in energy separations but the effect of various correlation potentials on f-band systems has not been studied

systematically. Nonetheless, one can say that this should cause their f bands to be lower and narrower rather than higher and broader.

D. Fermi surface

The intersections with symmetry planes of the calculated Fermi surface of La at the three lattice constants are shown in Fig. 6. The Fermi surface (FS) arises solely from band 2. Crudely speaking, the FS consists of large warped electron ellipsoids centered at the X points with the major axes aligned with the Γ-X directions. In the X-U-W plane, the $U(K)$ point is within the FS while the W point is outside. Instead of existing as three independent warped ellipsoids at the X points, however, necks extend along (at ambient pressure), or through (at $P=50$ and 120 kbar), the L-U-W-K planes which connect the various ellipsoids. The apparent electron pocket in the L-U-W-K plane at $P=50$ and 120 kbars in Fig. 6 is, in fact, a cross section of one neck. Thus the FS is a single, complicated, multiply connected sheet.

In addition, in the pressure range 50–120 kbars we find that a saddle point in band 2 along Γ-K crosses the Fermi level from above at 0.65 (1, 1, 0) $(2\pi/a)$. This band crossing, which is shown in detail in Fig. 7, results in a yet more complicated connectivity of the FS above the critical pressure at which the FS topology change occurs. We discuss this in relation to the 53-kbars transition in La in the next section. It should also be noted that another change in FS topology occurs in the range 0–50 kbars, where the necks mentioned above change their character due to a band crossing in the L-U-W-K plane. Implications of this FS change will also be discussed below.

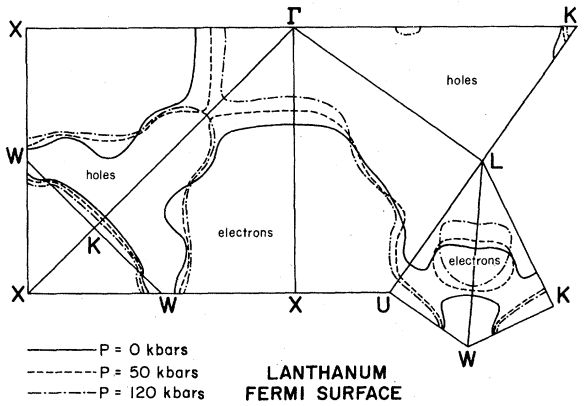

FIG. 6. Fermi surface of fcc La in the symmetry planes at 0, 50, 120 kbars pressure. Note the changes of topology under pressure in the L-K-W-U plane in the range 0–50 kbars, and along the Γ-K line in the range 50–120 kbars. (Obtained from a 65-parameter symmetrized Fourier-series fit to 128 band-2 eigenvalues in the IBZ.)

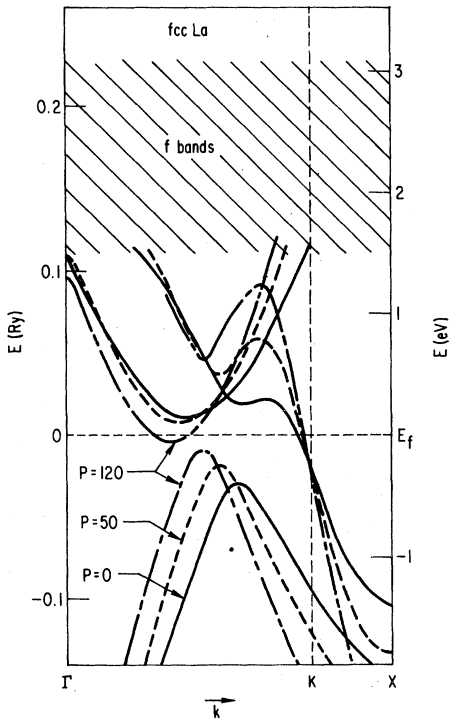

FIG. 7. Large-scale plot of the band structure of La along the Γ-K-X direction under pressure. It is actually a saddle point which crosses the Fermi level E_F at (0.65, 0.65, 0) $(2\pi/a)$.

The FS of Fig. 6 at zero pressure appears to be similar to the multiply connected FS reported by Myron and Liu[19] but not presented in detail by them. The FS's of TK and Glötzel and Fritsche[20] (GF) also were not discussed. From the band-structure plots of GF, discrepancies with the FS of Fig. 7 are apparent, however. At $P=0$, GF find that band 2 cuts the FS in three places along the Γ-K line, reminiscent of our results at P = 120 kbars. They also find that the band-1 maximum along Γ-K crosses E_F under a pressure of 120 kbars. Although we find that this maximum indeed increases under pressure, it is clear that it does not cross E_F in our calculations. It should be kept in mind that GF did not report their lattice constant corresponding to "$P=120$ kbars," and if it were significantly smaller than our value this discrepancy could be resolved.

IV. ISOSTRUCTURAL TRANSITIONS

Lifshitz[24] observed that when a change in FS topology occurs as a result of varying some parameter, which we take to be the pressure P, the electronic free energy F_e is nonanalytic in $E_m - E_F \equiv z$ at $z=0$ [E_m is the band feature (minimum,

saddle point, or maximum) which passes through E_F]. Explicitly, F_e can be written

$$F_e(P) = F_0(P) + \delta F(P), \tag{5}$$

where F_0 is analytic and δF contains nonanalytic terms in $z^{5/2}(P)$ and $T^{5/2}$ on one side of the transition. This behavior of δF arises from the electronic density of states which must have the general (three-dimensional) form $N(E) = N_0(E) + \delta N(E)$, with

$$\delta N(E) \propto |E - E_m|^{1/2} \tag{6}$$

on one side E_m. The form for δF alluded to above leads to discontinuities in second derivatives and to singularities in third derivatives[24] at $z(P) = 0$ and $T = 0$, and can be classified following Ehrenfest as a "$\frac{5}{2}$-order" transition. For simplicity we will refer to P_0 satisfying $z(P_0) = 0$ as the transition point, although the transition *at finite temperature* actually will occur slightly away from this point where dP/dV becomes *positive* and an isostructural phase transition occurs.[23]

This "Lifshitz transition" has been attributed as being responsible for a number of phase transitions, for example, the 42.5-kbars transition in Cs (Ref. 32), and it alone might account for structural instability in La. However, Dagens[25] has pointed out that, when electron-lattice coupling is taken into account, the *lattice* free energy contains a nonanalytic part containing $z(P)^{3/2}$ and $T^{3/2}$. Therefore this transition of "$\frac{3}{2}$ order" becomes stronger in that it occurs in lower derivatives. But, as mentioned above, the actual transition at $T \neq 0$ generally does not occur exactly at $z(P) = 0$ but only close to it.

One may consider another interesting possibility. Suppose the phase transition due to the electronic terms alone would occur at $z(P) = z_e$, and that due to the lattice alone would occur at z_l with $z_e \neq z_l$ in general. Under pressure the first condition to be satisfied could be either $z(P) = z_e$ (strictly a Lifshitz transition) or $z(P) = z_l$ (Lifshitz-Dagens transition). Accordingly the transition is referred to as due to electronic or lattice instability, although in either case the underlying dynamic mechanism is electronic in origin.

Considering the accuracy of the band-structure calculations and the predicted FS topology change in the appropriate pressure ranges, it seems very likely that the changes in FS topology are related to the 25- and 53-kbars transitions in La (Fig. 1). Furthermore, a number of observations suggest the Lifshitz-Dagens mechanism rather than a strictly Lifshitz instability for these transitions. First, since $\lambda(P=0) \geq 0.8$ (see Sec. V), and $T_c(50\ \text{kbars}) \simeq 10$ K suggests that λ increases under pressure, it is clear that the electronic system is strongly coupled to the lattice. This is also borne out by the calculations in Sec. V. Second, the relevant portions of the band structure are strongly hybridized (typically 50% d, 20% f, 30% sp), which in the rigid-muffin-tin approximation should lead to larger than average $|\Delta l| = 1$ contributions to electron-phonon coupling. Third, the FS changes occur at a general point at the zone boundary (low P) or along the $\langle 110 \rangle$ direction (high P), thus involving a rather large degeneracy factor as 24 (respectively, 12) inequivalent saddle points pass through E_F.

Since very little of a detailed nature is known about the phonon spectrum of fcc La, it is impossible to calculate free energies and confirm that either transition is of the Lifshitz-Dagens type. It is also difficult to verify experimentally the driving mechanism. Either type of instability will involve a (perhaps drastic) softening of the phonon spectrum at long wavelength in line with the $\vec{q} = 0$ nature of the transition. Such softening as well as anomalous ultrasonic attenuation could be checked by ultrasonic measurements under pressure. In addition, the squeezing off of several necks of FS on one side of the transition will result in a dramatic increase in the electronic density response function at many wave vectors; for the $\langle 110 \rangle$ instability the wave vectors are $\vec{q}_1 = (\tau, \tau, 0)$, $\vec{q}_2 = 2\vec{q}_1, \vec{q}_3 = (2\tau, 0, 0)$, and $\vec{q}_4 = (2\tau, \tau, \tau)$ in the IBZ, which connect the Fermi level crossings at $\vec{k} = (\tau, \tau, 0)$ and symmetry-related wave vectors [$\tau = 0.65(2\pi/a)$]. This indicates that a general softening of the phonon spectrum throughout the zone may occur. Phonon softening has been suggested[1] to be the cause of the "extra" increase in $T_c(P)$, at the transitions at 25 and 53 kbars, over the assumed smooth increase due to electronic causes, shown in Fig. 1 by dashed lines. Phonon softening up to ~15 kbars has been seen in tunnelling spectra,[33] and some phonon softening has even been inferred theoretically by Glocker and Fritsche[34] by comparing measured $T_c(P)$ values with calculated superconducting parameters. These aspects of superconductivity in La will be discussed further in the next section.

The 25-kbars transition at low temperatures is often stated in the literature to be the La dhcp $\rightleftarrows$ fcc structural transformation. In such a case this band crossing could be intimately related to the stability of the fcc phase. However, in a pressure-resistance study of the fcc La_xCe_{1-x} alloy series, King and Harris[23] have found the 25-kbars transition to be *continuously connected to the* $\gamma \rightleftarrows \alpha$ *isostructural* (fcc $\rightleftarrows$ fcc) *transition* at 7 kbar in Ce at room temperature. This result implies that the 25-kbars transition in La is also, at least in part, an isostructural transition. In

addition, King and Harris have noted that, if it were solely a dhcp ⟷ fcc structural transition, adding Ce to La would be expected to shift the transition to zero pressure at the point where the fcc phase becomes the thermodynamically stable phase, i.e., well before 100% Ce is reached. That this does not happen, and that a change in FS topology in La occurs in the same pressure region, suggests that a FS instability may drive this transition. Clearly more experimental work on this alloy series would help in understanding this behavior.

The 53-kbars transition at low temperature is usually assumed[1] to be an isostructural transition, primarily because the room-temperature structure is known[2] to be fcc in a wide pressure region 30–120 kbars. Interestingly, no discontinuity in lattice constant is observed at room temperature,[2] suggesting (1) a continuous (or nearly so) transition at low temperature or (2) the existence of a critical point in the range $100 < T < 300$ K. Again more experimental information is necessary to clarify the nature of this phase transition.

V. DENSITY OF STATES $N(E_F)$ AND THE SUPERCONDUCTING CRITICAL TEMPERATURE

The most striking property of La is its enormous increase in T_c under pressure, as shown in Fig. 1. In this section we present the results of theoretical calculations of quantities determining T_c, discuss in detail their behavior under pressure, and compare with the experimental data.

A. Theory: The rigid-muffin-tin approximation

McMillan[35] has shown that the electron-phonon coupling constant λ can be decomposed as

$$\lambda = \frac{N(E_F)\langle I^2\rangle}{M\langle\omega^2\rangle} \equiv \frac{\eta}{M\langle\omega^2\rangle}, \tag{7}$$

where $\langle I^2\rangle$ is the mean-square electron-ion matrix element, M is the ionic mass, and $\langle\omega^2\rangle$ is an appropriately defined mean-square phonon frequency (see below). The product $N(E_F)\langle I^2\rangle = \eta$ is an electronic stiffness constant, whereas $M\langle\omega^2\rangle$ reflects the stiffness of the lattice.

We have evaluated η in the rigid-muffin-tin approximation (RMTA) of Gaspari and Gyorffy,[36] which leads to the expression

$$\eta = \frac{2E_F}{\pi^2 N(E_F)} \sum_l (l+1)\sin^2(\delta_l - \delta_{l+1})\nu_l\nu_{l+1}. \tag{8}$$

Here $\nu_l \equiv N_l(E_F)/N_l^{(1)}(E_F)$, where $N_l^{(1)}(E_F)$ is the "single-scatterer" density of states defined by Gaspari and Gyorffy. In the RMTA it is assumed that the change in potential when an atom moves is given, in the muffin-tin region, by rigidly displacing the spherical potential, and in the interstitial region the change in potential is zero. This approximation has been used with considerable success in transition elements[37,38] for calculating T_c and the electrical resistivity, which involves similar electron-phonon matrix elements. The success of the RMTA, which makes a simple *ad hoc* assumption to avoid the complex screening problem, is a result of two occurrences in transition metals: (1) the change in potential is very large inside the muffin tin and is apparently rather well described by a rigid shift of the potential and (2) the wave functions at E_F are primarily d like and are strongly peaked inside the muffin tin, and therefore give little weight to the change in potential in the interstitial region. Unfortunately, these effects are not present in La, which is early in the 5d series, to the extent that they are in the middle or later d elements in the series. This is evident in Fig. 5, which shows that *neither* the d nor f radial function at E_F is strongly confined to the muffin-tin region (neither are the s and p radial functions). Thus we do not expect the RMTA to be as accurate in La as might otherwise have been expected.

It should also be noted that Eq. (8) was derived in a nonrelativistic approximation, whereas the densities of states $N_l(E_F)$ we have calculated and displayed in Table VI are from a fully relativistic theory. We have not attempted to generalize Eq. (8) to its relativistic analog, since spin-orbit effects are small in La. We use for the phase shifts δ_l the j-weighted average of δ_κ for $\kappa = l$ and $\kappa = -l - 1$.

In Table VI we list the phase shifts δ_l and the crystalline enhancement of the density of states ν_l up to $l = 4$, and $\sin^2(\delta_l - \delta_{l+1})$ and $\eta_{l,l+1}$ up to and including the $l = 3 \longleftrightarrow 4$ transition contributions. The p-d and d-f contributions to η dominate for all three lattice constants, approximately in the ratio 3:2. This is partly due to the strongly enhanced values of ν_1 and ν_3 (2.40 and 2.95 at ambient pressure, respectively). The approximately linear increase of η with pressure (or with decreasing volume) is mainly the result of an increased p-d contribution in the 0–50 kbars range and an increased d-f contribution in the 50–120 kbars range. However, both increases can be accounted for by the broadening of the various angular momentum scattering "resonances" under pressure. First note that ν_2 is relatively constant under pressure, so roughly

$$\eta \propto [E_F/N(E_F)]\,[\nu_1\sin^2(\delta_1 - \delta_2) + \nu_3\sin^2(\delta_2 - \delta_3)]\,. \tag{9}$$

TABLE VI. Phase shifts δ_l in radians, density-of-states ratios ν_l, $\sin^2$ factors and contributions $\eta_{l,l+1}$ to η in eV/Å^2.

		La			Y[a]	Y[b]	Sc[b]
	l	$a=10.0378$	9.4760	9.0340	(bcc)	(fcc)	(bcc)
δ_l	0	−0.959	−1.172	−1.309	−0.473	−0.703	−0.648
	1	−0.477	−0.620	−0.724	−0.140	−0.261	−0.172
	2	0.562	0.598	0.625	0.470	0.468	0.440
	3	0.025	0.036	0.047	0.0028	0.005	0.003
	4	0.0003	0.0005	0.0007			
ν_l	0	0.655	0.644	1.083	0.145	0.316	0.121
	1	2.397	2.026	1.654	2.409	2.100	4.449
	2	1.404	1.283	1.318	1.906	1.396	1.843
	3	2.945	2.250	2.649	5.756	3.851	4.943
	4	6.075	5.991	6.051			
$\sin^2(\delta_l-\delta_{l+1})$	0	0.215	0.275	0.305	0.107	0.183	0.210
	1	0.743	0.881	0.952	0.328	0.444	0.330
	2	0.262	0.284	0.299	0.203	0.199	0.179
	3	0.0006	0.0013	0.0021			
$\eta_{l,l+1}$	0	0.102	0.167	0.303	0.006	0.048	0.036
	1	1.519	2.138	2.300	0.541	1.024	1.719
	2	0.986	1.149	1.733	1.199	1.266	1.554
	3	0.013	0.032	0.076			

[a] From W. H. Butler, Ref. 37.
[b] From D. A. Papaconstantopoulos *et al.*, Ref. 38.

Since $\delta_l < \frac{1}{2}\pi$ for each l, broadening of the resonances results in larger values of $\delta_l - \delta_{l+1}$, and thereby increases the scattering strength $\sin^2(\delta_l - \delta_{l+1})$. This effect is especially evident in the p-d contribution at 120 kbars, where $\delta_1 \simeq \frac{1}{4}\pi$, $\delta_2 \simeq \frac{1}{4}\pi$ resulting in $\sin^2(\delta_1 - \delta_2) = 0.95$. *In the lower-pressure region,* the decrease of ν_1 cancels the increasing prefactor $E_F/N(E_F)$ and the increase in $\sin^2(\delta_l - \delta_{l+1})$ from 0.74 to 0.88 leads to an increase in η. The cancellation of the $\sin^2(\delta_l - \delta_{l+1})$ factor with $N_l^{(1)}$ in the denominator noted by Butler[37] (for $l=2$) does not occur here since it holds true only near the l resonance. *In the high-pressure regime,* the increase in η arises primarily from the increase in ν_3, which may reflect the increased width of the f resonance and/or increased d-f hybridization.

Also shown in Table VI is the f-g contribution $\eta_{3,4}$ to η in La, which reaches the still small but appreciable value 0.076 at high pressure. This is apparently the first time an f-g contribution to η has been reported. This value of $\eta_{3,4}$ is probably 1–2 orders-of-magnitude larger than in other transition metals, since δ_3 is 3–10 times larger in La, δ_4 is always negligible, and the product $\nu_3\nu_4$ is probably similar. It is interesting to note that the enhancement $\nu_4 = 6$ in La is similar[37,38] to ν_3 in Y and Sc, while ν_3 in La is reduced by a factor of 2–3 by a larger value of $N_3^{(1)}(E_F)$ from its value in Y and Sc.

It has long been a puzzle why La is such a good superconductor when the isoelectronic elements Y and Sc are very poor superconductors. The difference probably is not due entirely to structure since La superconducts at almost 5 K in the dhcp phase. It is also not a density-of-states effect, as all three show very large electronic specific-heat coefficients (see below). In Table VI we also show the corresponding parameters of "bcc Y" calculated by Butler[37] and of "fcc Y" and "bcc Sc" calculated by Papaconstantopoulos *et al.*[38] Considering the substantial differences between bcc Y and fcc Y, these results should not be taken too literally, especially in any comparison to experiment. Generally two differences between La and Y, Sc can be seen. The enhancement factors ν_l are smaller in La, due probably to larger bandwidths, or in the case of $l=4$, a larger single-scatterer density of states. This difference is offset by a larger $\sin^2(\delta_l - \delta_{l+1})$ factor in La, due primarily to a larger δ_2 which again arises from a larger bandwidth. The p-d contribution in La is also enhanced by a larger value of $|\delta_1|$ which is difficult to interpret but may be due to relativistic effects. As a result η(La) is not radically different from η(Y) and η(Sc) (in the cubic approximation), and

in fact lies midway between them. The corresponding values of λ and T_c will be discussed below. We note that the values of η reported here are (10–15 %) corrections to the preliminary results reported earlier.[39] We have also calculated the "nonspherical" d-f contribution to η and found it to be ~2% of the spherical contribution $\eta_{2,3}$. This contribution, which has not been included in the tables or discussion, is similar to that found for Y by Butler.[37]

B. Phonon spectrum

Rigorously, λ is a dimensionless measure of the strength of the electron-phonon spectral function α^2F given by

$$\lambda = 2\int_0^\infty \frac{d\omega\,\alpha^2F(\omega)}{\omega}. \tag{10}$$

Owing to the form of the electron-phonon matrix elements[35] occuring in α^2F, the first moment of α^2F is independent of the phonon spectrum and is equal to $\eta/2M$,

$$\eta = 2M\int_0^\infty d\omega\,\omega\alpha^2F(\omega). \tag{11}$$

From Eqs. (7), (10), and (11), $\langle\omega^2\rangle$ is the second moment of the phonon spectrum with respect to the weighting function $(2/\lambda\omega)\alpha^2F$,

$$\omega_2^2 \equiv \langle\omega^2\rangle = \int_0^\infty d\omega\,\frac{2}{\lambda\omega}\,\alpha^2F(\omega)\omega^2. \tag{12}$$

Allen and Dynes[40] have shown that, in a wide variety of metals, T_c is given accurately by λ, μ^*, ω_2 and another phonon average $\omega_{\log}$,

$$\log\omega_{\log} \equiv \int_0^\infty d\omega\,\frac{2}{\lambda\omega}\,\alpha^2F(\omega)\log\omega. \tag{13}$$

The Coulomb pseudopotential μ^* will be assumed to be 0.13 for the calculations described below. Although changes in T_c can be appreciable, our *conclusions* are not very sensitive to reasonable changes in μ^*.

Measurements of α^2F in La by tunnelling have been reported by Lou and Tomasch[41] and by Wühl, Eichler, and Wittig,[33] with some differences in their results. More important for the present discussion, it is likely that these α^2F spectra are more typical of dhcp La than fcc La[41] and inversion of the tunnelling spectra to obtain α^2F results in unrealistically small (or negative) values of μ^* and, probably, underestimates of λ. Accordingly we have used the phonon density-of-states function $F(\omega)$ for fcc La reported by Nücker,[42] assuming a constant $\alpha^2(\omega)$, to calculate the necessary phonon moments ω_2 and $\omega_{\log}$ shown in Table VII. [Nücker has shown that Lou and Tomasch's α^2F function satisfies $\alpha^2(\omega) \simeq$ constant over the energy region where F is large.] However, to check the differences between using F and α^2F, we have calculated ω_2 and $\omega_{\log}$ from the data of Lou and Tomasch.[41] We find $\omega_2 = 80$ K, $\omega_{\log} = 65$ K, which is roughly 10% softer than the values in Table VII obtained using $F(\omega)$. This is in accord with speculation[41] that La tunnelling spectra underestimate the high-frequency processes contributing to α^2F.

For Y, which we desire to compare with La, we have taken moments calculated by Butler[37] using $F(\omega)$ obtained from a Born–von Kármán force constant fit to the measured dispersion relations[43] of Y. Since the dispersion curves for Sc (Ref. 44)

TABLE VII. Parameters determining the superconducting transition temperature T_c in La under pressure, and in Y and Sc. Y and Sc should be compared with the ambient pressure ($a = 10.0378$ a.u.) parameters of La. The behavior of the phonon spectrum of La under pressure is unknown, and to assess variation of T_c with η, the phonon averages ω_2, $\omega_{\log}$ have been taken to be constant.

		fcc La			Y[a]	Y[b]	Sc[b]
		$a = 10.0378$	9.4760	9.0370	(bcc)	(fcc)	(bcc)
$N(E_F)$	(Ry spin)$^{-1}$	13.74	11.02	10.68	18.86	10.94	16.02
η	(eV/Å^2)	2.62	3.49	4.41	1.92	2.34	3.31
ω_2	(K)	86	86	86	149[c]	149[c]	226[d]
$\omega_{\log}$	(K)	74	74	74	132[c]	132[c]	200[d]
$M\langle\omega^2\rangle$	(eV/Å^2)	1.84	1.84	1.84	3.51	3.51	4.08
λ_{th}		1.42	1.90	2.40	0.55	0.67	0.81
$T_{c,\text{theor}}$	(K)	8.3	11.6	14.5	1.5	3.1	7.8
$T_{c,\text{expt}}$	(K)	6.05	10.0	11.6	(0.0006)[e]	(0.0006)[e]	0.0

[a] $N(E_F)$ and η taken from W. H. Butler, Ref. 37.
[b] $N(E_F)$ and η taken from D. A. Papaconstantopoulos *et al.*, Ref. 38.
[c] Calculated by W. H. Butler (Ref. 37) from inelastic neutron scattering data.
[d] Scaled from Y (see text).
[e] Extrapolated from alloy data; see Refs. 37 and 53.

are very similar to those of Y, we have simply scaled the moments of Sc by the difference in high-temperature values of Debye temperature to obtain the values listed in Table VII.

C. Determination of λ and T_c

From the electronic specific-heat coefficient[45] $\gamma = (\frac{1}{3}\pi^2)k_B^2(1+\lambda_\gamma)N(E_F)$ of fcc La, we obtain a total mass enhancement $\lambda_\gamma = 1.42$. It is now recognized that the electron-electron contribution λ_e to λ_γ may not be negligible[46] in transition metals. We expect, however, the value of λ_γ given above to be a near upper bound of the phonon enhancement λ. The corresponding values obtained from hcp band-structure calculations are $\lambda_\gamma = 1.20$ for Y (Ref. 47) and $\lambda_\gamma = 0.75$,[48] 1.01 (Ref. 49) for Sc.

In Table VII the calculated values of λ for La under pressure and for "cubic" Y and Sc are presented. We have supposed $M\langle\omega^2\rangle$ is constant under pressure to allow us to evaluate the change in λ and T_c which would result from the change in η alone. Wühl, Eichler, and Wittig[33] have detected softening of low-frequency modes and hardening of high-frequency modes in La up to 17.5 kbars which may result in a small net decrease in ω_2 and $\omega_{\log}$. Unfortunately there is no experimental information on the phonon spectrum in the high-pressure region.

At ambient pressure we calculate $\lambda = 1.42$, giving $T_c = 8.3$ K, which is too large by 2 K. Although this is not such a bad agreement considering the approximations which are made, we can investigate the effect of various corrections to the calculation. Assuming ω_2, $\omega_{\log}$, and μ^* are correct, $\lambda = 1.15$ is needed to reproduce $T_c = 6.0$ K. Papaconstantopoulos *et al.*[38] have advocated including "non-muffin-tin effects and screening" approximately by halving the d-f contribution to η. This somewhat *ad hoc* correction gives the intriguing result $\lambda = 1.15$ and hence the observed T_c. Assuming instead that η, ω_2, and $\omega_{\log}$ are correct, we can use the prescription of Bennemann and Garland[50] (BG) for μ^*, which can be rewritten

$$\frac{\mu^*_{\max}}{\mu^*} = 1 + \frac{N_0}{N(E_F)}, \tag{14}$$

with $\mu^*_{\max} \equiv 0.26$ and $N_0 \equiv 1$ (eV atom)$^{-1}$. This leads to $\mu^* = \mu^*_{BG} = 0.18$ (not 0.08 as reported by BG) and $T_c = 6.6$ K, again in much better agreement with experiment.

However, from the definition[40]

$$1/\mu^* = 1/\mu + \ln(\omega_{el}/\omega_{ph}), \tag{15}$$

where μ is the (dimensionless and unrenormalized) Coulomb potential, we can insert the maximum phonon energy[42] $\omega_{ph} = 13$ meV and electronic plasma energy $\omega_{el} \approx 6$ eV to put an upper bound on reasonable values of μ^*. An absolute upper bound, $\mu^* < 0.163$, results from considering the limit $\mu \to \infty$; this limit is lower than for most other transition metals because of the extreme softness of the phonon spectrum. For probable values of $\mu \lesssim 2$, we find $\mu^* \lesssim 0.15$, and the value $\mu^* = 0.13$ we have used in calculating T_c corresponds to $\mu \approx 0.7$. Thus our theoretical overestimation of T_c does not result from an underestimate of μ^* as the BG formula would suggest.

Finally, one could assume η and μ^* are correct as given above and scale ω_2 and $\omega_{\log}$ to reproduce the measured T_c. However, since we believe the phonon moments to be the most accurately determined quantities in the T_c equation, this could be misleading and we have not done this calculation. Considering the radial behavior of the $l = 2, 3$ wave functions shown in Fig. 5, we consider it fairly certain that the RMTA overestimates η by ~25%, and that some fundamental improvement beyond the RMTA in the electron-ion matrix element is necessary before a more precise picture of La can be obtained.

Since the phonon spectrum is being treated as constant under pressure, the increase in λ is parallel to the increase of η discussed above. The resulting increase in T_c indicates that the increase in η with pressure can easily explain the large value of dT_c/dP in this pressure range as long as the lattice does not stiffen too much. More generally, the behavior of T_c versus pressure shown in Fig. 1 then can be understood if significant phonon hardening under pressure does not occur below pressures of the order of 75–100 kbars.

In Fig. 8 we show the calculated pressure dependence of η compared with that of Glocker and Fritsche[34] and the $P = 0$ value of Glötzel.[21] The agreement between the three calculations is good, considering the use by these authors of a rigid-atomic-sphere approximation rather than the

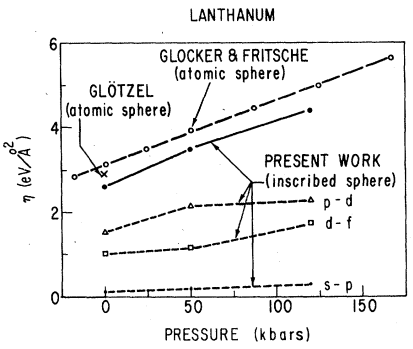

FIG. 8. Pressure behavior of η compared with calculations of Glocker and Fritsche (Ref. 34) and Glötzel (Ref. 21).

RMTA we have used. Glocker and Fritsche have used their calculated values of η for pressures of 0–150 kbars, together with the Allen-Dynes equation, to extract an empirical average phonon frequency Ω under pressure from measured values of T_c (Fig. 1). They made two simplifying assumptions: (1) that μ^* is given by the BG formula[50] ($\mu^* = 0.18$), and (2) $\omega_{\log} = \omega_2 \equiv \Omega$. Some relation between $\omega_{\log}$ and ω_2 must be assumed, since only one quantity can be determined from the T_c equation. As noted above, $\mu^* = 0.18$ is probably too large, but it was not crucial in determining the *behavior* of $\Omega(P)$. They found that in the range 30–55 kbars, Ω is 10% softer than at ambient pressure, and only for $P > 70$ kbars does the lattice harden linearly with pressure, with $d\Omega^2(P)/dP \approx 0.3$ meV^2/kbars. This indirect determination remains the best evidence of the lattice stiffness under pressure.

As noted above, η in cubic Y and Sc is similar to that of La, with the result that much of the large difference in λ and T_c is due to the extremely soft phonon spectrum of La. A similar conclusion has been reached previously[51,52] but on the basis of the Debye temperatures alone. Both λ and T_c are overestimated in Y and Sc, but, as was the case in La, much of this can be ascribed to difficulties with the RMTA. The severe overestimate of T_c in Sc may indicate that the cubic approximation also may be unreasonable. Assuming the phonon moments are reasonable, to account for the lack of superconductivity in Sc $\lambda \lesssim 0.30$ or a considerably larger μ^* is necessary, or possibly electron-electron interactions are not negligible. Whatever the case, the difference in T_c between Y, Sc, and La is no longer a complete mystery, but it is coupled with the equally complex question of the cause of the lattice softness. An obvious possibility (see below) is that the phonon frequencies are renormalized downward[16] by virtual transitions into the high density of unoccupied f states 2.5 eV above E_F. Such renormalization effects would result in a general, nearly $\vec{q}$-independent softening of the phonon spectrum. Another possibility is that the important renormalization arises from transitions nearer the Fermi surface, such has been found by Varma and Weber[53] in Nb. In the latter case, particularly good candidates for strong renormalization are phonons corresponding to the inter-saddle-point scattering wave vectors $\vec{q}_1$, $\vec{q}_2$, $\vec{q}_3$, $\vec{q}_4$ mentioned above. Clearly inelastic neutron scattering on a single crystal fcc La could test the predictions of these models.

The remaining puzzle is the cause of the large specific-heat mass enhancements $\lambda_\gamma = 1.2$ in Y and 0.75 to 1.0 in Sc. Compensating for the likely overestimate of η by the RMTA and the cubic approximation, it seems that there remains an electron-electron mass enhancement of the order of 0.75 in Y and of at least 0.25 in Sc. In analyzing specific-heat data at high temperatures where the phonon mass enhancement vanishes, Knapp and Jones[54] also found an apparent electron-electron mass enhancement, over band structure values, of 0.6 in Y and 0.4 in Sc. This is in quite satisfactory agreement with our estimates, considering the uncertainties. There also have been theoretical speculations[55] that spin fluctuations (of the antiparamagnetic type) might contribute to the mass enhancement in this region of the Periodic Table, but no convincing theory for such an effect exists at present.

VI. GENERALIZED SUSCEPTIBILITY

The generalized susceptibility $\chi(\vec{q})$ is defined (with n the band index) by

$$\chi(\vec{q}) = 2\sum_{\vec{k}nn'} \frac{f(\epsilon_{\vec{k},n}) - f(\epsilon_{\vec{k}+\vec{q},n'})}{\epsilon_{\vec{k}+\vec{q},n'} - \epsilon_{\vec{k},n}} , \tag{16}$$

and, as the name implies, is a measure of a general susceptibility of the electron system to respond to static perturbations or fluctuations of wave vector $\vec{q}$. This susceptibility has been correlated in various systems with magnetic transitions, structural transitions, and phonon anomalies. In light of the changes in Fermi-surface topology which result from saddle points crossing E_F under pressure, it becomes interesting to see whether any structure exists in $\chi(\vec{q})$ for values of $\vec{q}$ which connect these saddle points.

We have calculated the intraband contribution from band 2 to χ for $\vec{q}$ along the (100), (110), and (111) symmetry directions, using the tetrahedron method of Rath and Freeman.[56] Band 2 was represented (without the spin-orbit corrections to the eigenvalues, which are typically no greater than 1 mRy at E_F) by a 65-term Fourier series which was least-squares fit to 128 eigenvalues with an rms error of ~1 mRy. In the BZ integration, 1024 equal-volume tetrahedra in the IBZ were utilized.

The results are shown in Fig. 9 for ambient pressure, 50 and 120 kbars. Since $\chi(\vec{q} \to 0) \to N(E_F)$, which decreases under pressure, and since χ scales inversely with an energy denominator, the general decrease in χ under pressure reflects the broadening of the bands discussed in Sec. III. The wave vectors $\vec{q}_1$, $\vec{q}_2$, and $\vec{q}_3$, which span inequivalent saddle points at the $(\tau, \tau, 0)$ points which cross E_F between 50 and 120 kbars, are shown in Fig. 9. A difference plot (not shown) of $\chi(\vec{q}, 50\text{ kbars}) - \chi(\vec{q}, 120\text{ kbars})$ does show structure near each of these wave vectors: peaks near $\vec{q}_1$ and $\vec{q}_3$ and a

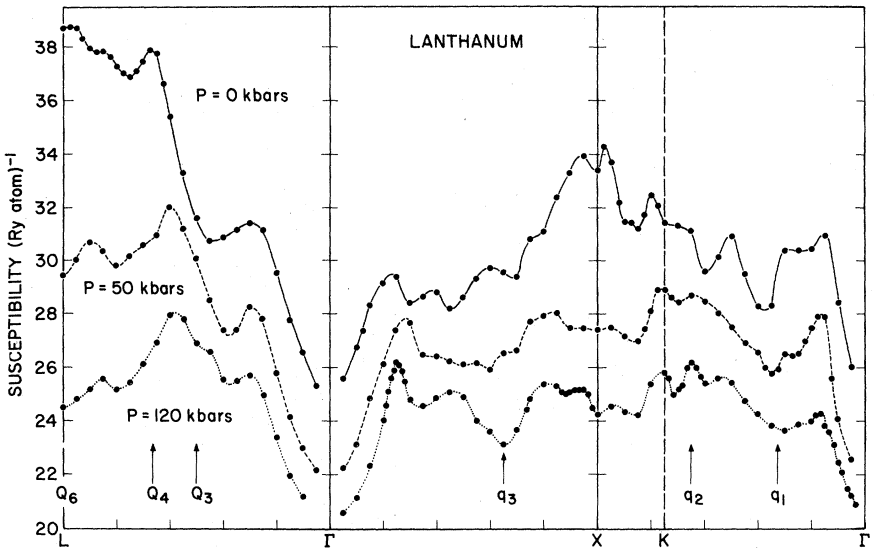

FIG. 9. Generalized susceptibility $[\chi(\vec{q})]$ of La along the three principal symmetry directions for the three lattice constants studied. The vector positions marked q_1, q_2, q_3 are the saddle-point vectors discussed in the text. The vector positions Q_3, Q_4, and Q_6 are the vectors relevant to the fcc to dhcp transition. The dramatic dip in $\chi(\vec{q})$ about the center of the zone Γ is quite pronounced (cf. text).

dip at $\vec{q}_2$. The structure is surprisingly sharp but also is rather small, and in any case does not approach becoming an absolute maximum. This should not be too surprising, since Dagens[25] has shown that χ is nonsingular as a function of $\vec{q}$, but is *discontinuous as a function of pressure* at the transition point. The sharp shoulders at $\vec{q}_1$ and $\vec{q}_3$ in χ(50 kbars) may be related to this discontinuity.

The dominant feature in $\chi(\vec{q}, P)$, which is apparent in Fig. 9, is the large increase is susceptibility along the Γ-L line which occurs as the pressure is *decreased from* 120 kbars. Since an increasing χ signifies a growing tendency towards an instability of the fcc phase, this behavior may be related to the fcc-dhcp instability at low pressure. With an appropriate choice of origin, the atomic displacements $\vec{\Delta}_i$ which are necessary to transform an fcc crystal to a dhcp crystal can be written

$$\vec{\Delta}_i \propto \hat{e}_1(2\cos\vec{Q}_4\cdot\vec{r}_i - 3\cos\vec{Q}_6\cdot\vec{r}_i) + \hat{e}_2(\sqrt{3}\sin\vec{Q}_3\cdot\vec{r}_i - 2\sin\vec{Q}_4\cdot\vec{r}_i), \quad (17)$$

where $\hat{e}_1$ and $\hat{e}_2$ are unit vectors parallel to the $[1\bar{1}0]$ and $[11\bar{2}]$ directions, respectively, $\vec{Q}_j = (\frac{1}{12}j)\,(2\pi/a)\,(1,1,1)$ and $\vec{r}_i$ denotes a lattice site in the fcc crystal. The wave vectors $\vec{Q}_3$, $\vec{Q}_4$, and $\vec{Q}_6$ are shown in Fig. 9, where the drastic increase in $\chi(\vec{Q}_4)$ and $\chi(\vec{Q}_6)$ under reduced pressure is evident. This correlation strongly suggests an instability toward a charge-density wave described by $\vec{\Delta}$, which could result in an fcc-to-dhcp structural transition.

This interpretation complements the suggestion of Fleming, Liu, and Loucks[18] (FLL) that the Fermi surface is responsible for the stability of the dhcp structure, relative to hcp in La. FLL noted that the heavier rare-earth metals which have the hcp structure have very flat pieces of Fermi surface perpendicular to the c direction and about half-way between Γ and the zone boundary. They argued that La, by assuming the dhcp structure, creates a Fourier component of the crystal potential which destroys these flat pices of Fermi surface and thereby substantially reduces the electronic energy.

Finally we note another somewhat anomalous feature of the susceptibility curves of Fig. 9, namely, the sharp drop in χ inside a region of radius $\sim 0.4(\pi/a)$ surrounding Γ. This reflects relatively fewer low-energy small-wave-vector electron-hole excitations compared to more ordinary susceptibility curves which tend to be rather flat near Γ. As a result the phonon-dispersion curves can be expected to show more dispersion in the range $|\vec{q}| < 0.4(\pi/a)$ than in metals with "normal" susceptibilities near Γ.

VII. DISCUSSION

A. Band structure and f electrons

The present calculations of the electronic structure of La show clearly the characteristics of the f bands: They lie about 2.5 eV above E_F and rise and broaden moderately under pressure. The

primary uncertainty in our calculation involves the choice of correlation functional. As mentioned in Sec. II, the initial effect (for example, in a self-consistency loop) of using a functional corresponding roughly to a larger value of α, as is often done, would be to lower the f bands relative to the d and sp bands, since they lie primarily in a region of higher charge density. However, due to the large occupation-number dependence of the f bands, the resulting increase in f charge in turn will raise the f bands. Therefore the effect of the large *intra-atomic Coulomb correlation* is to decrease the influence of the correlation functional on the f bands. For this reason there is probably rather little uncertainty introduced into our results by using this specific local-density functional.

As a result of hybridization, we find approximately 0.05–0.10 *localized* f electron in the range 0–120 kbars. This is an insignificant amount compared to the 0.7 f electron[11] or "occupied f band"[1,10] which has been postulated to account for the low melting point and high-temperature superconductivity of La. However, *in terms of the electronic configuration*, i.e., $(sd)^3$, La is a typical transition metal. An important way in which it differs from Sc and Y is that unoccupied f bands lie ~ 2.5 eV above E_F, with the concomitant additional virtual d-f excitations from the valence bands into the f bands, i.e., f-like density fluctuations.

Because of these additional virtual excitations the phonon spectrum is renormalized to lower frequencies.[16] (A study of this effect is in progress.) That a softer lattice accounts for much of the difference in superconducting properties has been shown in detail in the previous section. The softer lattice also accounts approximately for the decreased melting temperature T_M of La relative to Y and Sc, by the following consideration. The average phonon occupation number at T_M, $[\exp(\omega_2/T_M)-1]^{-1} \simeq T_M/\omega_2$, is roughly 10 in La where $T_M = 920$ K. For Y and Sc, with $T_M \approx 1800$ K and ω_2 again taken from Table VII, the phonon occupation numbers at the melting point are 12 and 8, respectively. Therefore La melts when its phonon population is similar to that of Y and Sc at their melting temperatures. In other words, Lindemann's law holds here, as indeed it does across the trivalent rare earths. It is unnecessary to invoke *occupied* f bands, as was done by Matthias *et al.*[11] and Wittig and collaborators,[1,10] to account for lanthanum's superconductivity and low melting point. It has also been conjectured[11] that the dhcp structure itself is indicative of significant f occupation in La, as this structure occurs primarily in f-electron systems (rare earths and actinides). Recent work by Duthie and Pettifor[57] however, indicates that the dhcp structure can be accounted for without reference to f electrons.

These same arguments probably can be extended to metallic La compounds unless charge transfer off the La atoms occurs. In such compounds we expect the La f bands to remain *essentially* unoccupied, although slight f occupation arising from hybridization may affect certain features (e.g., the Fermi surface[58]). An example of such a system which has similarities to the La, Y, Sc, and Lu series is that of the C15 compounds XAl_2. $LaAl_2$ has $T_c = 3.24$ K while its Sc, Y, and Lu counterparts do not become superconducting above 1 K, and the latter compounds have $M\langle\omega^2\rangle$ factors which are larger[59] by 35% or more, assuming $\langle\omega^2\rangle \propto \theta_D^2$. Another example is provided by the CsCl structure compound[60] LaAg where $T_c = 0.94$ K, while YAg and LuAg do not become superconducting above 0.33 K. Other examples of C14, C15, $D10_2$, $L1_2$, DO_{11}, and DO_{19} have been discussed by Smith and Luo.[60] A striking *counterexample* to these trends (which deserves further study) is provided by the examination of the simple cubic hexaborides by Fisk,[61] who finds YB_6 to have $T_c = 7$ K while LaB_6 has $T_c = 0.122$ K.

Another feature of the electronic spectrum of La which has attracted speculation is the f bandwidth and its pressure dependence. We have found a bandwidth of the order of 1 eV which increases by roughly 50% under 120-kbars pressure. These numbers (see Table III) depend on how one chooses to define the bandwidth; we note however that the f bandwidth and center *at* Γ agrees very well (to within 5 mRy) with the Wigner-Seitz criteria of vanishing and diverging logarithmic derivatives at the extreme of the bands. Through hybridization with the broad d bands there is an appreciable density of f states at E_F (see Table IV) which is 2.5 eV below the center of the f bands. An important consideration here is how this bandwidth arises, whether from crystal fields, direct f-f overlap or from hybridization. The crystal-field possibility can be dispensed with quickly. The tests leading to the results of Table V show that the crystal fields (nonspherical potential inside the muffin-tin sphere, "warping" terms in the interstitial region) have a very small effect on the relative separation of the extreme of the f bands. Crystal fields are, of course, generally smaller in metals than in semiconductors and insulators due to the presence of metallic screening. In addition, at both Γ and X the f bands are uncoupled from other angular momentum components, ruling out hybridization as an important factor in determining the bandwidth. (Of course, at general wave vectors the f partial density of states is non-

zero over a larger "hybridization bandwidth" than is being considered here.)

The roughly 1-eV average f bandwidth therefore arises from direct f-f overlap, as would be expected when the Wigner-Seitz criteria predict the band extrema so well. The ordering of the levels at Γ is also consistent with this picture and with our earlier observation that the f states tend toward a nonbonding character. Recall that the lowest f state at Γ, $\Psi(\Gamma_{2'})$, is 70 and 150 mRy lower than $\Psi(\Gamma_{15})$ and $\Psi(\Gamma_{25})$, respectively (Table V). By pointing along the $\langle 111 \rangle$ directions $[\Psi(\Gamma_{2'}) \sim xyz]$ rather than toward nearest or next-nearest neighbors, $\Psi(\Gamma_{2'})$ is able to assume the maximum "bonding-like" character (lowest energy, most spatially extended, and least kinetic energy) without actually having to form an appreciable interatomic f-f σ-bonding state. The Γ_{15}, and especially the Γ_{25}, states point toward neighboring atoms and consequently their eigenvalues are raised by the nonbonding (or perhaps antibonding) character of the f states.

B. Resistivity

Bloch-Grüneisen theory, based on the semiclassical Boltzmann equation, predicts that the electrical resistivity $\rho(T)$ should behave linearly with T, $\rho(T) = \rho_0 + \rho_1 T$, in metals above θ_D. Lately it has become evident[62] that many high-temperature superconductors show a marked deviation from linearity, often referred to as "saturation". The interpretation is controversial with a recent review having been given by Allen.[63] However, it has been found that a parallel resistor formula

$$\rho(T)^{-1} = (\rho_0 + \rho_1 T)^{-1} + \rho_{\max}^{-1}, \tag{18}$$

often provides an excellent fit to the experimental data over a wide range of independent variation of the temperature and the disorder resistivity ρ_0 (especially in A15 compounds[62,64]). We note two important facts concerning this expression. The temperature coefficient ρ_1 can be calculated reliably[64,65] from band-structure calculations and an estimate of λ from the superconducting transition temperature. Secondly, $\rho_{\max}$, which is interpreted as the maximum (or saturation) resistivity, seems to be more or less constant[62,64] within a class of materials which may exhibit quite widely varying properties. These properties suggest that Eq. (18) has a fundamental significance beyond a mere empirical fit.

The experimental resistivity of predominantly fcc La, measured by Alstad *et al.*,[66] shows a negative deviation from linearity above $\theta_D \sim 120$ K, up to room temperature $T_R = 300$ K, the maximum temperature measured. Since La is a good superconductor, this behavior is not surprising. We have fit, by a least-squares procedure, the measured $\rho(T)$ to Eq. (18). A good fit was obtained with $\rho_1 T_R = 129$, $\rho_{\max} = 211$ $\mu\Omega$ cm. We can also calculate ρ_1 from band-structure quantities[64]

$$\rho_1 T = 4\pi/\Omega_p^2 \tau_{ep}, \tag{19}$$

$$\Omega_p^2 = \tfrac{4}{3}\pi e^2 N(E_F) v^2(E_F), \tag{20}$$

$$1/\tau_{ep} = 2\pi\lambda_{tr} k_B T/\hbar, \tag{21}$$

if the electron-phonon transport coupling constant λ_{tr} is known. Our calculated values of the mean-square Fermi velocity $v^2(E_F)$ and plasma energy $\hbar\omega_p$ for La at three values of the lattice constant are given in Table VIII. It has been found[65] that $\lambda_{tr} \cong \lambda$ is often a good approximation. We use this assumption here with the value $\lambda = 1.15$ which is necessary to account for the observed T_c. The calculated value of $\rho_1 T_R = 138$ $\mu\Omega$ cm compares favorably with the value of 129 $\mu\Omega$ cm from the empirical fits.

The value of $\rho_{\max}$ which we find is relatively small for an element, even slightly smaller than the value of 230 $\mu\Omega$ cm found for Nb (Ref. 62) ($T_c = 9.2$ K). For Lu (Ref. 67), for example, where deviation from linearity in $\rho(T)$ is obvious up to the melting point, we find $\rho_{\max} \sim 400$ $\mu\Omega$ cm. For A15 compounds, however, where $T_c \sim 20$ K for some members, $\rho_{\max} \simeq 130$–150 $\mu\Omega$ cm.[62,64] At present there is no clear theoretical understanding of this constant parallel resistivity, if indeed it is in any sense fundamental. A generalization of transport theory by Chakraborty and Allen[68] to include nonclassical interband scattering suggests $\rho_{\max}$ may arise from an interband polarizability and may be related to the temperature dependence of the band structure. There is no evidence, however, that the unoccupied f bands in La play any fundamental role in causing saturation behavior.

The phonon-limited mean free path of the electrons is given by

$$l_{ep} = \hbar v(E_F)/(2\pi\lambda_{tr} k_B T). \tag{22}$$

At room temperature $l_{ep} = 10$ Å, i.e., La at room temperature is *approaching* the condition $l = a$ which is expected when clear saturation behavior is observed. Assuming that any contribution ρ_i to the resistivity arises from a corresponding con-

TABLE VIII. Calculated rms Fermi velocity $v(E_F)$ (in 10^7 cm/sec) and plasma energy $\hbar\Omega_p$ (in eV) for three values of the lattice constant a (a.u.).

a	$v(E_F)$	$\hbar\Omega_p$
10.0378	2.67	3.17
9.4760	3.09	3.58
9.0340	3.34	4.09

tribution $1/\tau_i$ to the total scattering rate $1/\tau$ according to Eq. (19), it follows from $l = v(E_F)\tau$ that ρ_{max} is associated with a minimum (saturation) mean free path $l_{min} = 4.5$ Å, which corresponds closely to the lattice constant $a = 5.3$ Å. A similar agreement between l_{min} and a holds for Nb (Ref. 62) and for A15 compounds.[64] Indeed, the logical extension of this argument implies, for a metal of lattice constant a, a maximum resistivity given by

$$\rho_{max} = (3/e^2)/[N(E_F)v(E_F)a] . \quad (23)$$

This can be interpreted as a generalization of the reciprocal of the nearly-free-electron formula of Mott and Davis[69] for their minimum metallic conductivity. We have not investigated whether this expression can be justified from experimental data for other systems besides La, Nb, and A15 compounds.

C. Thermal anomalies

In this paper we have studied primarily the effects of pressure on the low-temperature (i.e., ground-state) properties of La. However, some interesting thermal anomalies (besides the resistivity) have been observed in La. Andres[9] found a negative thermal-expansion coefficient in the range $T_c < T < 38$ K in a predominantly fcc sample. He noted further that such behavior in a nonmagnetic metal is highly unusual, having previously been found only to occur in the diamond-structure elements C, Si, and Ge. Eliseev *et al.*[9] also found a region of large negative thermal expansion above room temperature. In addition, the Knight shift[7] and magnetic susceptibility[6] show considerable variation in the range $0 < T < 300$ K.

The temperature variation of the Knight shift and susceptibility, especially in high-temperature superconductors, is often interpreted in terms of thermal smearing of fine structure in the electronic density of states. This would be an especially attractive explanation in La, because Varley[70] has shown that smearing of fine structure can also lead, in certain cases, to a negative thermal-expansion coefficient. Although we find an exceptionally sharp and comparatively large peak in $N(E)$ near E_F in Fig. 3, it is too far above E_F (5 mRy $\simeq$ 750 K) to lead to any significant temperature variation at low temperature. In addition, the slope $[dN(E)/dE]_{E=E_F} \simeq 14$ Ry^{-2}atom^{-1} is 2 *orders-of-magnitude smaller* than in (for example) Pd,[71] where it seems to be agreed that temperature broadening is a primary source of thermal anomalies.

Andres has pointed out on the basis of lattice dynamics and thermodynamics, that a negative thermal-expansion coefficient can result from shear modes which soften under pressure. In view of the observation with tunnelling of low-frequency-phonon softening[15] under pressure (albeit in presumably dhcp material), this explanation seems the most probable at present.

ACKNOWLEDGMENTS

The authors acknowledge several helpful conversation with T. Jarlborg. W.E.P. would like to thank B. Chakraborty for discussions on transport theory. This work was supported by the AFOSR, Grant No. 76-2948 and by the U. S. Department of Energy.

*Permanent address: Naval Research Laboratory, Washington, D. C. 20375.

[1]H. Balster and J. Wittig, J. Low Temp. Phys. 21, 377 (1975).

[2]K. Syassen and W. B. Holzapfel, Solid State Commun. 16, 533 (1975).

[3]J. Kondo, Prog. Theor. Phys. 29, 1 (1963).

[4]D. C. Hamilton and M. A. Jensen, Phys. Rev. Lett. 11, 205 (1963); C. G. Kuper, M. A. Jensen, and D. C. Hamilton, Phys. Rev. 134, A15 (1964).

[5]C. F. Ratto, B. Coqblin, and E. Galleani d'Agliano, Solid State Commun. 7, 1387 (1969); B. Coqblin and C. F. Ratto, Phys. Rev. Lett. 21, 1065 (1968).

[6]J. M. Lock, Proc. Phys. Soc. London B70, 566 (1957).

[7]W. E. Blumberg, J. Eisinger, V. Jaccarino, and B. T. Matthias, Phys. Rev. Lett. 5, 51 (1960).

[8]D. H. Parkinson, F. E. Simon, and F. H. Spedding, Proc. R. Soc. London A207, 137 (1951); D. L. Johnson and D. K. Finnemore, Phys. Rev. 158, 376 (1967).

[9]A. A. Eliseev *et al.*, Russ. J. Inorg. Chem. 9, 565 (1964); K. Andres, Phys. Rev. 168, 708 (1968).

[10]J. Wittig, Comments Solid State Phys. 6, 13 (1974).

[11]B. T. Matthias, W. H. Zachariasen, G. W. Webb, and J. J. Engelhardt, Phys. Rev. Lett. 18, 781 (1967).

[12]A. S. Edelstein and A. M. Toxen, Phys. Rev. Lett. 17, 196 (1966); J. J. Hauser, *ibid.* 17, 921 (1966); H. J. Levinstein, V. G. Chirba, and J. E. Kunzler, Phys. Lett. 24A, 362 (1967); A. S. Edelstein, Phys. Rev. 164, 510 (1967); J. S. Rogers and S. M. Khana, Phys. Rev. Lett. 20, 1284 (1968).

[13]L. Y. L. Shen, in *Superconductivity in d- and f-Band Metals*, edited by D. H. Douglas (AIP, New York, 1972), p. 31.

[14]L. F. Lou and W. J. Tomasch, Phys. Rev. Lett. 29, 858 (1972).

[15]H. Wühl, A. Eichler, and J. Wittig, Phys. Rev. Lett. 31, 1393 (1973).

[16]F. Weling, Solid State Commun. 26, 913 (1978).

[17]E. A. Kmetko, in *Electronic Density of States*, edited by L. H. Bennett [Nat. Bur. Stand. (U.S.), Spec. Publ. 323, Washington, D. C., 1971], p. 67.

[18]G. S. Fleming, S. H. Liu, and T. L. Loucks, J. Appl.

Phys. 40, 1285 (1969).
[19]H. M. Myron and S. H. Liu, Phys. Rev. B 1, 2414 (1970).
[20]D. Glötzel and L. Fritsche, Phys. Status Solidi B 79, 85 (1977).
[21]D. Glötzel, J. Phys. F 8, L163 (1978).
[22]T. Takeda and J. Kübler, J. Phys. F 9, 661 (1979).
[23]E. King and I. R. Harris, J. Less-Common Met. 27, 51 (1972).
[24]I. M. Lifshitz, Zh. Eksp. Teor. Fiz. 38, 1569 (1960) [Sov. Phys.—JETP 11, 1130 (1960)].
[25]L. Dagens, J. Phys. (Paris) Lett. 37, L37 (1976); J. Phys. F 8, 2093 (1978).
[26]D. D. Koelling and B. N. Harmon, J. Phys. C 10, 3107 (1977).
[27]D. D. Koelling and G. O. Arbmann, J. Phys. F 5, 2041 (1975).
[28]A. H. MacDonald, W. E. Pickett, and D. D. Koelling, J. Phys. C 13, 2675 (1980).
[29]N. Elyashar and D. D. Koelling, Phys. Rev. B 13, 5362 (1976); 15, 3620 (1977); N. Elyashar, Ph.D. thesis, University of Illinois, Chicago, 1975 (unpublished). Relativistic theory is discussed by M. E. Rose, *Relativistic Electron Theory* (Wiley, New York, 1961).
[30]W. E. Pickett, A. J. Freeman, and D. D. Koelling (unpublished).
[31]S. P. Kowalczyk, Ph.D. thesis, University of California, Berkeley, 1976 (unpublished); Y. Baer and G. Busch, Phys. Rev. Lett. 31, 35 (1973); P. Steiner, H. Höchst and S. Hüfner, J. Phys. F 7, L145 (1977).
[32]A. K. McMahan, Phys. Rev. B 17, 1521 (1978); S. G. Louie and M. L. Cohen, *ibid.* 10, 3237 (1974).
[33]H. Wühl, A. Eichler, and J. Wittig, Phys. Rev. Lett. 31, 1393 (1973).
[34]R. Glocker and L. Fritsche, Phys. Status Solidi B 88, 639 (1978).
[35]W. L. McMillan, Phys. Rev. 167, 331 (1968).
[36]G. D. Gaspari and B. L. Gyorffy, Phys. Rev. Lett. 28, 801 (1972).
[37]W. H. Butler, Phys. Rev. B 15, 5267 (1977).
[38]D. A. Papaconstantopoulos *et al.*, Phys. Rev. B 15, 4221 (1977).
[39]W. E. Pickett, A. J. Freeman, and D. D. Koelling, in *Superconductivity in d- and f-Band Metals*, edited by H. Suhl and M. B. Maple (Academic, New York, 1979).
[40]P. B. Allen and R. C. Dynes, Phys. Rev. B 12, 905 (1975).
[41]L. F. Lou and W. J. Tomasch, Phys. Rev. Lett. 29, 858 (1972).
[42]N. Nücker, in Prog. Rep. of Teilinstitut Nukleare Festkörperphysik, Inst. f. Angewandte Kernphysik, Ges. f. Kernforschung Karlsruhe, KFK No. 2538, 1977 [Prog. Rep. of Nucl. Solid State Physics, Appl. Nucl. Phys. Inst., Soc. Nucl. Phys., Karlsruhe, KFK No. 2538, 1977] (unpublished).
[43]S. K. Sinha, T. O. Brun, L. D. Muhlestein, and J. Sakurai, Phys. Rev. B 1, 2430 (1970).
[44]N. Wakabayashi, S. K. Sinha, and F. H. Spedding, Phys. Rev. B 4, 2398 (1971).
[45]D. L. Johnson and D. K. Finnemore, Reference 8.
[46]A value of $\lambda_e \simeq 0.4$ ($=\lambda_e+\lambda_p$ in their notation) was suggested for Pd by F. M. Mueller, A. J. Freeman, J. O. Dimmock, and A. M. Furdyna, Phys. Rev. B 1, 4617 (1970). Recent de Haas-van Alphen experiments give a value of $\lambda_e \simeq 0.2$ for Nb; see G. W. Crabtree, D. H. Dye, D. P. Karim, D. D. Koelling, and J. B. Ketterson, Phys. Rev. Lett. 42, 390 (1979); H. Rietschel and H. Winter, Phys. Rev. Lett. 43, 1256 (1979).
[47]T. L. Loucks, Phys. Rev. 144, 504 (1966).
[48]S. G. Das, A. J. Freeman, D. D. Koelling, and F. M. Mueller, in *Magnetism and Magnetic Materials*, edited by C. D. Graham (AIP, New York, 1973), p. 1304.
[49]G. S. Fleming and T. L. Loucks, Phys. Rev. 173, 685 (1968).
[50]K. H. Bennemann and J. W. Garland, in *Superconductivity in d- and f-Band Metals*, edited by D. H. Douglas (AIP, New York, 1972), p. 103.
[51]T. Satoh and T. Ohtsuka, J. Phys. Soc. Jpn. 23, 9 (1967).
[52]T. Kasuya, in *Magnetism*, edited by G. T. Rado and H. Suhl (Academic, New York, 1966), Vol. II B, p. 252–259.
[53]C. M. Varma and W. Weber, Phys. Rev. Lett. 39, 1094 (1977); Phys. Rev. B 19, 6142 (1979).
[54]G. S. Knapp and R. W. Jones, Phys. Rev. B 6, 1761 (1972).
[55]Discussions of the effects of spin fluctuations in metals have been given by N. F. Berk and J. R. Schrieffer, Phys. Rev. Lett. 17, 433 (1966); S. Doniach and S. Engelsberg, *ibid.* 17, 750 (1966); K. H. Bennemann and J. W. Garland (Ref. 50).
[56]J. Rath and A. J. Freeman, Phys. Rev. B 11, 2109 (1975).
[57]J. C. Duthie and D. G. Pettifor, Phys. Rev. Lett. 38, 564 (1977).
[58]E. Seitz, B. Lengeler, G. Kamm, and J. Kopp, J. Phys. 40, C5-76 (1979); T. Jarlborg and A. J. Freeman (unpublished).
[59]R. E. Hundsberg and K. A. Gschneidner, J. Phys. Chem. Solids 33, 401 (1972).
[60]T. F. Smith and H. L. Luo, J. Phys. Chem. Solids 28, 569 (1967).
[61]Z. Fisk, quoted by A. J. Arko *et al.*, Int. J. Quantum Chem. 9, 569 (1975).
[62]H. Wiesmann, M. Gurvitch, H. Lutz, A. Ghosh, B. Schwarz, M. Strongin, P. B. Allen, and J. W. Halley, Phys. Rev. Lett. 38, 782 (1977), and references therein.
[63]P. B. Allen, in *Superconductivity in d- and f-Band Metals*, edited by H. Suhl and M. B. Maple (Academic, New York, 1979).
[64]P. B. Allen, W. E. Pickett, K. M. Ho, and M. L. Cohen, Phys. Rev. Lett. 40, 1532 (1978).
[65]F. J. Pinski, P. B. Allen, and W. H. Butler, Phys. Rev. Lett. 41, 431 (1978).
[66]J. K. Alstad, R. V. Colvin, S. Legvold, and F. H. Spedding, Phys. Rev. 121, 1637 (1961).
[67]B. Delley, H. Beck, H. U. Künzi, and H.-J. Güntherodt, Phys. Rev. Lett. 40, 193 (1978).
[68]B. Chakraborty and P. B. Allen, Phys. Rev. Lett. 42, 736 (1979); Phys. Rev. B 18, 5225 (1978); B. Chakraborty, Ph.D. thesis, SUNY, Stony Brook, 1979 (unpublished).
[69]N. F. Mott and E. A. Davis, *Electronic Processes in Noncrystalline Materials* (Oxford University, Oxford, England, 1971).
[70]J. H. O. Varley, Proc. R. Soc. London 237A, 413 (1956).
[71]See, for example, F. M. Mueller *et al.* (Ref. 46). More recent calculations have been reported by T. J. Watson-Yang, B. N. Harmon, and A. J. Freeman, J. Magn. Magn. Mater. 2, 334 (1976).